



DYNAMIC CONSTELLATION TASKING AND MANAGEMENT

THESIS

Steven P. Ingraham, Captain, USAF

AFIT-ENY-13-M-18

**DEPARTMENT OF THE AIR FORCE
AIR UNIVERSITY**

AIR FORCE INSTITUTE OF TECHNOLOGY

Wright-Patterson Air Force Base, Ohio

APPROVED FOR PUBLIC RELEASE; DISTRIBUTION UNLIMITED

The views expressed in this thesis are those of the author and do not reflect the official policy or position of the United States Air Force, Department of Defense, or the United States Government. This material is declared a work of the U.S. Government and is not subject to copyright protection in the United States.

DYNAMIC CONSTELLATION TASKING AND MANAGEMENT
THESIS

Presented to the Faculty

Department of Aeronautics and Astronautics

Graduate School of Engineering and Management

Air Force Institute of Technology

Air University

Air Education and Training Command

In Partial Fulfillment of the Requirements for the
Degree of Master of Science in Astronautical Engineering

Steven P. Ingraham, BS

Captain, USAF

March 2013

APPROVED FOR PUBLIC RELEASE; DISTRIBUTION UNLIMITED

DYNAMIC CONSTELLATION TASKING AND MANAGEMENT

Steven P. Ingraham, BS

Captain, USAF

Approved:

Jonathan T. Black, PhD (Chairman)

Date

Thomas Atwood, PhD (Member)

Date

Kerry D. Hicks, PhD (Member)

Date

Ronald J. Simmons, Lt Col, USAF
(Member)

Date

Abstract

Responsive orbits have gained much attention in recent years and many AFIT theses have addressed this topic. Specifically, the following topics have been studied: plane change maneuvers, phasing within an orbit, adjusting time of arrival, avoidance, and maneuver detection. This thesis seeks to determine the feasibility of maneuvering satellites from circular (600 km) orbits to eccentric (600 km by 175 km) orbits in order to collect high resolution images for Earth surveillance. Coverage is calculated for multiple 6-satellite constellations. Perturbations for the subject orbits are analyzed and compared to simulation results. ΔV requirements are determined to offset the differential perturbations between the circular and eccentric orbits. Additionally, the effects of atmospheric drag are modeled for solar maximum and solar minimum conditions. The ΔV required to offset atmospheric losses is also calculated. Finally, a hypothetical ΔV budget is quantified for a ten day operation and compared to the total ΔV available on the NanoEye concept. The results of this thesis show that maneuvering satellites within a constellation is feasible in order to obtain high resolution images. The ΔV budget for a hypothetical ten day scenario is found to be approximately 1.2 km/s.

Acknowledgments

I would like to thank my research advisor, Dr. Jonathan Black, and my committee for their guidance and support in my thesis effort. I would also like to thank the students in the Astronautical Engineering department who have taught me much along the way.

I am very grateful that I was selected to be a full-time Master's student while on Active Duty. I look forward to my future assignments and the challenges that will accompany. AFIT has taught me the skills to succeed and has provided me with countless contacts who should plan on hearing from me in the coming years.

Steven P. Ingraham

Table of Contents

	Page
Abstract	iv
Acknowledgments	v
List of Figures	ix
List of Tables	x
I. Introduction	1
1.1. Overview	1
1.2. Background	2
1.3. Assumptions	6
1.4. Scope	6
1.5. Methodology	7
1.6. Overview of Thesis	7
II. Literature Review	9
2.1. Introduction	9
2.2. Constellations in Use	10
2.3. Responsive Orbits / Responsive Constellations	14
2.4. DARPA SeeMe Concept	20
2.5. SMDC NanoEye Concept	21
2.6. Summary	23
III. Methodology	24
3.1. Introduction	24
3.2. Orbit Selection	25
3.3. Target Selection	27
3.4. Constellation Design	28

	Page
3.5. Coverage Geometry	29
3.6. Computer Simulation	32
3.7. Perturbations	33
3.8. Considerations for Eccentric Orbits	34
3.9. Evaluation Period	38
3.10. Summary	39
IV. Analysis and Results	40
4.1. Introduction	40
4.2. Inclination	41
4.3. Coverage Analysis	41
4.4. Constellation Coverage	43
4.5. Considerations for Eccentric Orbits	45
4.6. Phasing Maneuver	57
4.7. ΔV Budgets for Maneuvering	59
4.8. Revisiting Inclination	63
4.9. Example Scenario	71
V. Conclusions and Recommendations	77
5.1. Introduction	77
5.2. Inclination	78
5.3. Coverage	79
5.4. Constellation	80
5.5. Eccentric Orbits	82

	Page
5.6. Atmospheric Drag	84
5.7. ΔV Budgets	84
5.8. Significance of Research.....	85
5.9. Recommendations for Future Work.....	86
Appendix A.....	89
Appendix B	92
Appendix C	99
Appendix D.....	101
Bibliography	104

List of Figures

	Page
Figure 1. NanoEye Engineering Model	4
Figure 2. Walker Delta Constellation (3 planes / 2 satellites per plane).....	11
Figure 3. DARPA SeeMe Satellite (Artist's Concept)	20
Figure 4. NanoEye sketch with Components Labeled.....	22
Figure 5. Angular Geometry for Spacecraft with Elevation Angle Constraint.....	30
Figure 6. Swath Width and Ground Track Shown on Earth	31
Figure 7: RAAN Regression vs. Inclination	35
Figure 8. Apsides Rotation vs. Inclination.....	36
Figure 9: Apsides Rotation (Exaggerated).....	50
Figure 10: Apogee Altitude vs. Time for Circular and Eccentric Orbits.....	56
Figure 11: Apogee vs. Time (Showing Detail).....	57
Figure 12: Slant Range Histogram for Eccentric Orbits at 50.57° Inclination	65
Figure 13: Slant Range Histogram for Eccentric Orbits at 43.61° Inclination	65
Figure 14: DARPA ALASA (Artist's Concept)	81
Figure 15: STK Force Model (Atmosphere).....	91

List of Tables

	Page
Table 1: NanoEye Specifications	5
Table 2: CRISIS Specifications	17
Table 3: Possible Constellations	29
Table 4: Coverage Validation at 350 km	42
Table 5: Coverage Validation at 850 km	42
Table 6: Phasing Parameters	43
Table 7: Coverage for Circular Orbits Inclined to 50.57°	44
Table 8: RAAN Regression with J_2 and Inclination 50.57°	47
Table 9: RAAN Regression with HPOP and Inclination 50.57°	48
Table 10: Coverage for Eccentric Orbits at Inclination 50.57° (RAAN Drift, Symmetric)	49
Table 11: Coverage for Circular Orbits at Inclination 50.57° (RAAN Drift, Symmetric)	50
Table 12: Perigee Rotation with J_2 and Inclination 50.57°	51
Table 13: Perigee Rotation with HPOP and Inclination 50.57°	52
Table 14: Altitude Over Target Latitude as a Function of True Anomaly (ν) at Inclination 50.57°	53
Table 15: Apogee Altitude for Inclination 50.57°	55
Table 16: ΔV Required for Phasing Maneuver	59
Table 17: Daily ΔV Budget for Inclination 50.57°	59
Table 18: Running ΔV Total for 10 Days at Inclination 50.57°	60
Table 19: Running ΔV Total for 10 Days at Inclination 50.57° (RAAN Drift)	61

	Page
Table 20: ΔV Budget per Orbit for Inclination 50.57°	62
Table 21: Coverage for Circular and Eccentric Orbits at Inclinations 50.57° and 43.61°	64
Table 22: RAAN Regression with HPOP and Inclination 43.61°	67
Table 23: Perigee Rotation with HPOP and Inclination 43.61°	68
Table 24: Altitude Over Target Latitude as a Function of True Anomaly (v) at Inclination 43.61°	69
Table 25: Apogee Altitude for Inclination 43.61°	70
Table 26: Daily ΔV Budget for Inclination 43.61°	70
Table 27: Coverage for Eccentric Orbits at Inclination 43.61° (RAAN Drift, Symmetric)	71
Table 28: Coverage for Circular Orbits at Inclination 43.61° (RAAN Drift, Symmetric)	71
Table 29: Example Scenario: ΔV Budgets for Satellites 1a, 2a, and 3a	73
Table 30: Example Scenario: ΔV Budgets for Satellites 1b, 2b, and 3b	74
Table 31: Coverage Metrics for Example Scenario	75
Table 32: ΔV Budget for $i = 50.57^\circ$ (RAAN, Perigee, Atm)	93
Table 33: ΔV Budget for $i = 50.57^\circ$ (Perigee, Atm)	94
Table 34: ΔV Budget for $i = 50.57^\circ$ (RAAN, Atm)	95
Table 35: ΔV Budget for $i = 43.61^\circ$ (RAAN, Perigee, Atm)	96
Table 36: ΔV Budget for $i = 43.61^\circ$ (Perigee, Atm)	97
Table 37: ΔV Budget for $i = 43.61^\circ$ (RAAN, Atm)	98
Table 38: Minimum Slant Range to Target at Inclination 50.57°	99
Table 39: Minimum Slant Range to Target at Inclination 43.61°	100

	Page
Table 40: Coverage metrics for 12 Satellite Constellations at 50.57° Inclination.....	102
Table 41: Coverage metrics for 12 Satellite Constellations at 43.61° Inclination.....	103

DYNAMIC CONSTELLATION TASKING AND MANAGEMENT

I. Introduction

1.1. Overview

Constellations have been studied extensively in the past half century and are used by both civilian companies and government agencies to provide persistent satellite coverage of Earth. Recently, students at the Air Force Institute of Technology (AFIT) have explored the following concepts: maneuvering satellites to adjust the ground track so that a satellite pass can be coordinated to observe a particular point on Earth; delaying or advancing the time a satellite overflies such a target; and maneuvering a satellite to avoid a possible collision. A comprehensive study has not yet been published showing the implications of maneuvering individual satellites within a constellation.

This research will seek to answer the question: can a constellation of satellites in Low Earth Orbit (LEO) be used by tactical warfighters to collect images of battle space targets for near real-time decision making? A constellation of satellites will be modeled to provide non-continuous regional coverage. Maneuvering will be used to overfly targets at varying altitudes to satisfy necessary levels of imagery resolution. The initial deployment phase of this constellation is of prime interest. Analysis and modeling will be used to determine orbit and constellation design to maximize coverage metrics for a six satellite system. In order to provide frequent updates to the user, the two most important metrics to examine are number of accesses and revisit time.

1.2. Background

Awareness of the battle space has always been key to successful military operations. Aerial photography began in the late 1850s with cameras suspended by balloons and kites. In 1909, the first photographs were taken from an aircraft. In the early 1960s satellites began taking photographs and used reentry capsules to return the film to Earth (Campbell). Today, photographs captured by satellites are transmitted to Earth ground stations over satellite communication links. While information is travelling at the speed of light, the time it takes between requesting satellite imagery and then receiving a useable product is not instantaneous. The Army is attempting to allow tactical users to submit imagery requests directly to orbiting satellites and have the images sent to a mobile device in the field.

Currently, overhead imaging is provided by large satellites and Unmanned Aerial Vehicles (UAVs). Existing satellite systems are too few in number to offer constant coverage of the battlefield. Though UAVs are responsive, they are susceptible to air defense systems, airspace congestion, and Federal Aviation Administration (FAA) regulations. Their vulnerabilities make them impractical in conflicts against a technologically advanced adversary until air superiority is established. A large constellation of smaller, more agile satellites could provide data faster and more consistently than existing systems.

NanoEye is a proposed Earth surveillance satellite system designed to orbit between 175 km and 600 km altitude. The Army's Space and Missile Defense Command (SMDC) developed a concept of operations (CONOPS) to maneuver the NanoEye

satellites, to receive taskings directly from the tactical user, and to return data more quickly than has been observed in recent conflicts.

To achieve the levels of persistence and responsiveness desired, a great number of satellites are required. Several orbital planes, each comprised of multiple satellites, would form a constellation that revisits a target area frequently. Each satellite must be inexpensive in both production and deployment to compete with UAVs and prove to be affordable for the Army. The concept of small, low-flying satellites offers the best combination for minimizing total cost.

Image resolution has a linear relationship between optic size and orbital height; a 0.25 meter optic must orbit at approximately 175 km to achieve 0.5 meter resolution. This defines the orbit necessary to achieve National Image Interpretability Rating Scale (NIIRS) 6. Atmospheric drag at this altitude will quickly overcome the energy of the satellite and degrade the orbit to the point of re-entry. Therefore, it would be better to orbit above the atmosphere and maneuver, or “dip” into the atmosphere when sub-meter resolution is required. When high-resolution images are not required, the satellite orbits at approximately 600 km and provides 1.5 meter resolution.

The specifications for the NanoEye system set the foundation for this research (see Table 1). Though many of the system’s details have not been released publicly, enough information is available to study the implications of the proposed orbits and determine a constellation structure that maximizes the coverage of the system. The concept proposed by SMDC relies on a maneuvering satellite with propellant for over 2.5 km/s change in velocity (ΔV). With this maneuvering capability, the satellites can ascend and descend to achieve a desired image resolution, adjust the ground track through

phasing maneuvers, recover energy lost to atmospheric drag, and conduct stationkeeping for constellation management. When a satellite descends to low altitudes, atmospheric drag not only degrades the orbit, it also has the tendency to impart aero-torques on asymmetric bodies. For this reason the SMDC NanoEye design is symmetric about the velocity vector and the body mounted solar panels form a wedge pointing in the same direction (see Figure 1). SMDC expects the operational life of individual satellites to be approximately three years, but the exact lifespan would depend directly on the number of maneuvers performed and the amount of time spent in the atmosphere. A greater frequency of maneuvers will more quickly expend the propellant. When all of the propellant has been exhausted, a satellite can no longer add energy to offset drag and will eventually be overcome by the atmosphere and forced to reenter. Approximately 239 m/s ΔV is required to maneuver a satellite into an eccentric orbit with perigee at 175 km and then re-circularize the orbit at 600 km. The stationkeeping requirements will be determined and presented in the results chapter of this thesis.

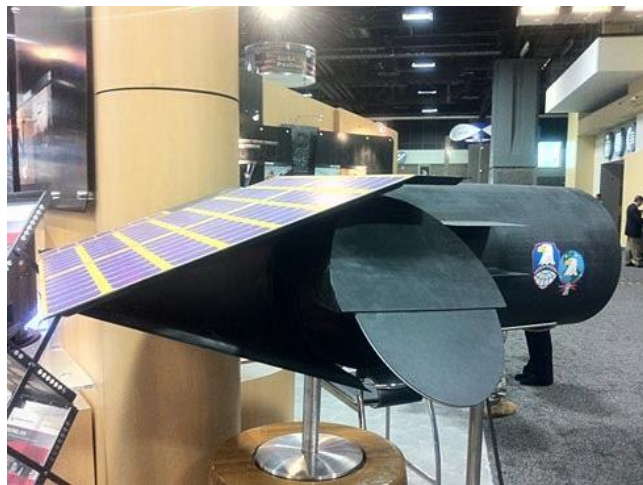


Figure 1. NanoEye Engineering Model

The following table summarizes the specifications envisioned by SMDC for the NanoEye satellite:

Table 1. NanoEye Specifications

Mass:	Dry mass of 20 kg / Wet mass of 80 kg
Sensor:	CMOS imaging sensor (16 frames per second and store 100 pictures)
Minimum working elevation angle:	20 degrees
Minimum field of view at nadir:	0.8 km x 0.8 km
Swath width at minimum/ maximum altitude:	500 km / 2000 km
Propulsion:	Propellant tank is the primary spacecraft structure; will use propellant to maneuver and de-orbit at end of life
S/C attitude control:	3 axis control by reaction wheels; magnetic torquers for desaturation
Orbital plane inclination:	3 to 5 degrees higher than the latitude of the target
Launch responsiveness:	24 hour requirement from garrison storage call up to launch ready

This thesis will investigate constellation design, satellite maneuverability, and constellation management to determine the feasibility of relying on numerous small satellites to augment “big space” and fill the gap in coverage that is currently provided by UAVs. “Big space” refers to the large and very expensive satellites used for Earth sensing and satellite communications. Often costing over \$1B each these satellites cannot be mass produced. A constellation of smaller, less expensive, satellites may prove to be more responsive to operational needs than typical “big space” assets.

1.3. Assumptions

In this research it is assumed that a method is in place to accurately track satellites and determine the orbits with high precision. The input to the model will be the Classical Orbital Elements (COEs) for each satellite.

It is also assumed that the main perturbations to the two-body orbital problem are air drag and the J_2 effect (equatorial bulge of the Earth). The computer program Satellite Tool Kit (STK) will be used for modeling and simulation. STK uses the High-Precision Orbital Propagator (HPOP) to step forward through time, given the satellite's COEs. The results of the STK analysis will give a reasonable estimate of the motion of the satellite in its orbit. When satellites are commanded to maneuver, it is assumed that the spacecraft thrusters will provide exactly the amount of thrust desired.

1.4. Scope

The first objective of this research is to determine what configuration of satellites maximizes coverage for the initial deployment of the constellation. The initial deployment will consist of six satellites. Six satellites is a reasonable starting point for a LEO surveillance constellation and may represent the first phase of a constellation containing more satellites. Multiple configurations will be examined to compare coverage characteristics for each. The orbit of a maneuvering satellite will be compared to that of a reference satellite (600 km circular) to determine the effects of perturbing forces on the altitude, Right Ascension of the Ascending Node (RAAN), the argument of perigee, and the true anomaly. Pertinent analysis that is not covered in this thesis will be recommended for future research.

1.5. Methodology

The approach for examining the feasibility of satellite maneuverability will be to calculate the theoretical ΔV required to maneuver between the circular (600 km) orbit and the eccentric (600 km apogee, 175 km perigee) orbit. Estimates for drag experienced will also be performed. The data will be processed to explore trends in orbit decay, in and out-of-plane drift, and constellation deformation. Stationkeeping requirements will be estimated and feasibility of the concept will be evaluated.

1.6. Overview of Thesis

The following chapter summarizes relevant research in the field of constellations, coverage, and responsive orbits. Substantial research in constellations began in the 1960s with J.G. Walker. Research has been steady over the past four decades and many fielded constellations are based on the concepts of Walker, Lang, and Adams and Rider.

Chapter 3 gives a detailed description of the methodology used to explore the SMDC NanoEye concept and how best to approach this constellation in the build-up phase. Chapter 3 is set up so that the method can be reproduced and carried on in further research.

Chapter 4 presents the results of the analysis. Coverage data and operational requirements are listed for multiple scenarios and the results are quantified to make mission planning decisions. The ΔV requirements for maneuvering, station-keeping, and orbit maintenance are compared to the benefits of such constellations as well as the risks associated with each approach.

Chapter 5 highlights the conclusions of the results and makes recommendations for implementation of the SMDC NanoEye constellation. It is foreseeable that the results of this study might be used in mission planning for similar constellations, especially for collecting images of Earth with high-resolution and high-frequency. This final chapter will also indicate areas for further research related to responsive constellations.

II. Literature Review

2.1. Introduction

This chapter provides a survey of relevant research from academic journals, conference proceedings, and government publications. A brief summary of relevant AFIT theses will also be discussed. The literature provides a foundation to explore aspects of maneuvering that have not yet been published. The implications of maneuvering an individual satellite within a constellation have impacts on the satellite's orbit as well as the constellation. This thesis will attempt to fuse together the perturbations to LEO orbits, the ΔV required to offset these perturbations, the effects on coverage if the perturbations are not counteracted, and finally make recommendations on the use of maneuvering satellites based on the total ΔV requirements. The literature review begins with a historical overview and works through basic concepts to allow for analysis of dynamic constellations.

A constellation is a group of satellites that work together to achieve a common objective. Global coverage is a common goal of constellation designers and many have proposed methods to achieve this with the minimum number of satellites. The first major breakthrough came in 1970 with a British publication by John G. Walker who proved that global coverage could be achieved using five satellites in his Delta configuration (Middour). In 1985, W.S. Adams and L. Rider focused on polar orbits to provide continuous global coverage of the Earth using a concept called "streets of coverage" (Middour). Thomas Lang explored the concept of using constellations for regional coverage, also called zonal coverage. Lang's constellations sought to provide continuous

coverage of a band of latitudes where the majority of the world's population resides (Lang, 1996). All of the concepts mentioned above utilize symmetric constellations. In symmetric constellations there are multiple orbital planes each containing at least one satellite, and all of the planes are inclined to the same degree. Additionally, each plane has the same number of satellites and all satellites orbit at a common altitude (Middour).

Knowledge of the following definitions will be helpful in understanding concepts addressed in the remainder of this thesis. *Continuous global coverage* provides access to at least one satellite from every point on Earth. *Regional coverage* and *zonal coverage* refer to a subset of the surface of the Earth that is of interest for satellite coverage. *Partial coverage* has access gaps, where a given point on Earth does not have access to a satellite at all times. *Revisit time*, in the case of partial coverage, is the time it takes for a satellite in the constellation to return to a given point on Earth for a subsequent observation. The basic principle of constellation design is to maximize coverage and minimize revisit time for regions of interest while using the minimum number of satellites.

2.2. Constellations in Use

The popularity of Walker constellations has endured over the past forty years and is currently used by the Global Positioning System (GPS), GLONASS, Globalstar, and other government and commercial satellite constellations.

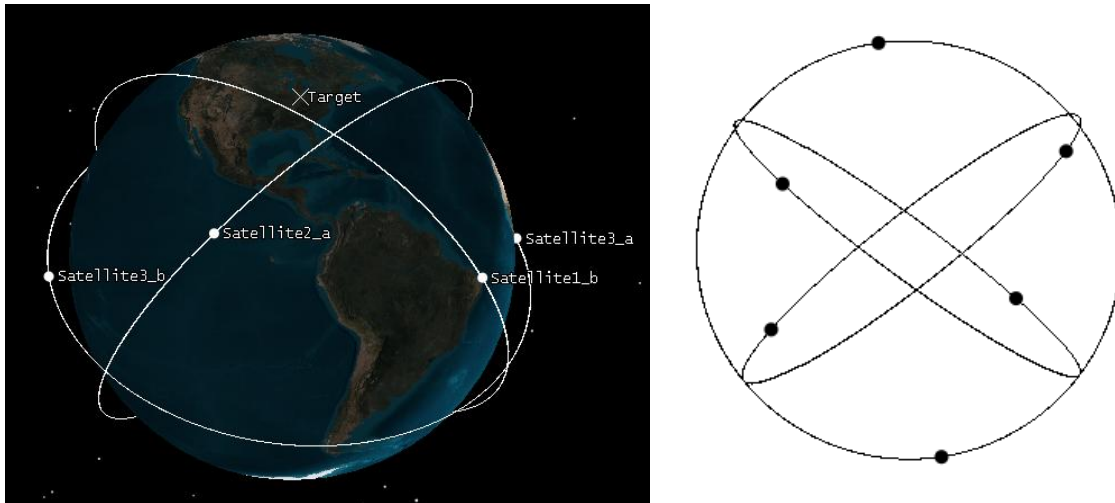


Figure 2. Walker Delta Constellation (3 planes / 2 satellites per plane)

In 1987, John Hanson reviewed the previous research in his article “Improved Low-Altitude Constellation Design Methods.” Coverage analysis for constellations using streets of coverage (polar orbits) must be performed at the equator because all satellites necessarily converge at higher latitudes. Regarding Walker constellations, Hanson examined the relative phasing of satellites in adjacent planes. He observed that although an optimal phasing exists with a particular number of satellites, other non-optimal phasings also exist that will provide similar coverage. Hanson asserts that the fewest number of satellites for coverage is achieved when only one satellite resides in each plane. This configuration is theoretically the best, but the concept of operations (CONOPS) for the launch of one satellite per plane is typically more expensive than launching multiple satellites into fewer planes. Multiple planes require either multiple launches or costly plane change maneuvers.

In his “Survey of Orbit Selection for Satellite Earth Surveillance,” Jay Middour reviewed much of the same material as Hanson. Middour states that no analytic method

is available for selecting optimal orbit parameters for partial coverage. Rather, numerical search techniques must be used to look for combinations of inclination, altitude, number of planes, and number of satellites per plane to meet performance requirements.

Alternatively, if coverage from multiple satellites is desired (V-fold coverage), a minimum of $2V+3$ satellites are required. This is consistent with Walker's claim that five satellites is the minimum number necessary to provide continuous single-fold global coverage. Middour reviewed and confirmed Lang's finding that Walker constellations are the most efficient design for constellations with less than 20 satellites. For applications using more than 20 satellites Adams Rider constellations are most efficient. A final point from this study is that only one mixed inclination constellation (non-symmetric) has been found to outperform a Walker constellation. These guiding principles will be used to help determine the most efficient constellation design for the NanoEye system.

In 2002, Andrew Turner developed a method for quickly computing the optimal phasing parameter (F) in the Walker notation. He finds that the phasing parameter can be found simply using:

$$F = (P - 1) - (T / P) \quad (1)$$

where P is the number of planes and T is the number of satellites. If F is negative, increase F by P until a positive value is obtained.

Turner's article also explores the concept of maneuvering, on-orbit servicing, and satellite refueling. Turner concludes that constellation designers should group multiple satellites in a common plane for more efficient on-orbit service calls. Also, even if

refueling were available, the ΔV required for satellites to perform out-of-plane maneuvers is expensive and therefore not feasible with current technology.

Olivier de Weck studied the concept of building constellations gradually, rather than deploying a full constellation at once. His inspiration comes from two commercial ventures that sought to capitalize on a customer base that never materialized. Iridium and Globalstar are constellations of LEO satellites for commercial communications, consisting of 66 and 40 satellites, respectively. Both parent companies filed for bankruptcy in 1999 after land-based cellular telephone networks provided a similar product at a lower cost to the user. de Weck proposes that flexibility should be designed up front to mitigate the risk of overbuilding space systems. The key concept is to reduce economic risk by matching users' needs with deployed capability. He proposes that the first wave of satellites serve as a technology demonstrator. Then, the initial constellation size is matched to the current demand. The initial satellites must carry additional propellant in order to maneuver if/when satellites join the constellation in order to optimize coverage. This flexibility increases the cost of the first deployment but would have saved the Iridium and Globalstar companies billions of dollars.

The literature reviewed thus far on constellation design provides a solid foundation for the topic to follow, responsive constellations. As the cost of developing and launching space systems decreases, it becomes feasible to use a greater number of smaller satellites in LEO constellations to complement the large, expensive satellites currently in use.

2.3. Responsive Orbits / Responsive Constellations

James Wertz (2005) provides an overview of five types of responsive orbits (Cobra, Magic, Sun Synchronous, Fast Access, and Repeat Coverage Orbits) and their uses. The most important qualities that make a responsive orbit useful are: low cost, good coverage, tactical applications, and responsiveness. It is assumed that long-term stability and global coverage are not of principal importance when considering responsive orbits; the emphasis is on responding to particular events in distinct regions.

Cobra and Magic Orbits are highly elliptical orbits that place apogee over a region of interest and loiter for prolonged coverage of that region, similar to a Molniya Orbit developed in the former Soviet Union. This is particularly useful for communications satellites, but the high altitude make them less useful for surveillance purposes. LEO Sun Synchronous Orbits provide coverage of targets in the same lighting conditions each day. Sun-synchronous orbits often find use in Earth imaging because image analysis is made easier by the steady conditions. The disadvantage of a polar orbit is that approximately 30% of the satellite's time is spent orbiting the Polar Regions where operations are unlikely to be required. Satellites in LEO Fast Access Orbits fly directly over a target on the first pass, similar to an intercontinental ballistic missile, but the trajectory is orbital rather than ballistic. LEO Fast Access Orbits observe the target and return to the vicinity of the launch point in one orbital period, on the order of 90 minutes, and are the fastest method to return data from a surveillance pass. LEO Repeat Coverage Orbits are inclined slightly higher than the target's latitude, three to five degrees, and provide approximately five minutes of coverage for four or five consecutive orbits per satellite, per day. Wertz states that with LEO Repeat Coverage Orbits three or four satellites could

provide coverage with a revisit time of 90 minutes and six or eight satellites could provide coverage with a revisit time of 45 minutes.

The combination of launch preparation time, weather delays, orbit insertion time, orbit response time, and data return time must all be considered if we wish to launch a satellite in response to a real-time event. All considered, the use of satellites to return data from remote regions in a responsive manner makes them a truly tactical asset.

Scott Larrimore quotes Lt. General Larry Dodgen to call for this tactical capability, “What the Army wants is persistent surveillance and the means to move that information around the battlefields.” Dodgen was the commander of Space and Missile Defense Command (SMDC) when he made this statement in 2004. With the goal of providing non-continuous regional coverage, Larrimore proposed to use orbits with inclinations slightly greater than the target latitude to increase the number of access opportunities. He also pointed out that orbital planes precess (about the Earth’s rotational axis), depending on altitude, eccentricity, and inclination. This perturbation is caused by the oblateness of the Earth (the equatorial bulge, termed J_2) and essentially causes a drift in the Right Ascension of the Ascending Node (RAAN) to the west for prograde orbits. This regression of the node affects the time of day the satellite ground track will intersect the target, but not the coverage performance of the orbit.

Jared Krueger, Daniel Selva, Matthew Smith, and John Keesee searched for a method to determine the optimal spacecraft and orbital characteristics to build a constellation whose purpose was collecting “high resolution imagery with nearly continuous coverage on short notice.” They refer to their notional satellite system as the Continuous Responsive Imaging System in Space (CRISIS). This constellation shares

many characteristics with the Disaster Monitoring Constellation (DMC), but with increased resolution and coverage; further discussion of the DMC is to follow.

Krueger's article identifies the following variables to be examined: orbit altitude, number of planes, number of satellites per plane, communications system, attitude determination and control system (ADCS), off-nadir satellite slewing angle (degrees), and payload sensor optical array size (number of pixels). There are 1350 combinations of these variables and a top-down approach to determine the optimal configuration is not possible. An integrated model was created to represent the spacecraft's parameters and simulate competing configurations. Outputs of the model are metrics of mass, cost, coverage, response time, and cost per image. The authors' methodology uses MATLAB to implement the model while STK and Simulink are used as interfaces to perform the analysis. The method calculates the metrics in two phases; first for individual satellites and then again for the constellation. The methodology used by the authors to analyze the trade space of constraining certain design parameters is Pareto analysis. Then, Pareto-optimal architectures are evaluated to arrive at the solution.

The inputs to Krueger's model are the system level requirements. CRISIS was expected to be launched on the Pegasus XL launch vehicle, having a payload fairing diameter of 1.15 meters. Other system level requirements are summarized in the table below:

Table 2. CRISIS Specifications

Ground Resolution	Less than or equal to 1.0 meter
Responsiveness	Mean Response Time less than or equal to 4 hours
Coverage	Between plus/minus 70 degrees latitude
Duration	No less than 1 year operational lifetime for constellation
Number of Targets	5 (Store and Download) or 1 (Realtime)
Mass	Approx 200 kg
Dimensions	Diameter less than or equal to 1.15 meters

The research and simulation determined that the system design should have the following parameters: the constellation will have two planes each containing four satellites, each satellite will orbit in a circular orbit at an altitude of 600 km, the off-nadir angle will be capable of reaching 40°, and the optical array will contain 10,000 pixels. The attitude control system will use a zero-momentum 3-axis method to provide sufficient pointing accuracy. Momentum wheels will not be used because the gyroscopic rigidity they impart on the spacecraft would hinder the slew rate required to be responsive to subsequent mission taskings. The system's cost divided by the expected operations tempo yields a cost per picture of approximately \$7,200. Additionally, the team recommends that an Evolved Expendable Launch Vehicle (EELV) Secondary Payload Adapter (ESPA) ring-type method be considered to launch multiple satellites, in a common plane, on a single medium lift launch vehicle.

In 2010, Eves and Taylor explored the advantages and disadvantages of using constellations as well as the methodology of current satellite design for the purpose of responsive constellations. The primary advantage of constellations is that they “bridge the gap” between the capabilities provided by large spacecraft and the tactical assets currently provided in theater. The authors argue that the surveillance data provided by manned and unmanned aircraft may be significantly reduced if the United States enters a conflict with a “near-peer” and air superiority is yet not established. Further, national assets in space would be likely targets for anti-satellite (ASAT) weapons in a large-scale conflict.

Satellite constellations provide benefits, but typically at a high cost. Eves and Taylor propose a new paradigm in satellite design to offset the total system cost. The typical dual-string (redundant) design of satellites could be discarded to decrease costs if we are willing to measure the reliability at the system level rather than focus on the reliability of each satellite. Mass production of satellites would also decrease the per-unit cost. However, if potential adversaries identified a vulnerability across the architecture they may be capable of taking the entire constellation offline with a single attack. For this reason, the authors propose maintaining a dual-string design in the command and control of the satellites, but accepting the risk of single-string in the other satellite subsystems.

Additionally, Eves and Taylor propose that the satellites work in two modes, normal and crisis. When a threat is detected by a single satellite, a warning message would go out to the rest of the constellation to transition to crisis mode and take defensive measures. This cross-link communication would increase the survivability of the

constellation, but attrition is still to be expected. The loss of a single satellite could be offset using on-orbit spares or by re-phasing the remaining satellites in the affected plane. The number of satellites that could be destroyed before compromising the mission would depend on the particular application. Generally, the region of coverage would not be affected but the percent of time the target receives coverage would decrease and the mean revisit time would increase. The overall goal is to allow individual satellites to be expendable while taking measures to preserve the constellation and its capabilities.

Hong, along with others, apply many of the concepts discussed above to a current satellite system, the DMC. This constellation is a multinational effort to provide persistent coverage of the Earth for disaster recovery efforts. The current system is designed so that individual satellites (each under different ownership) collect data and compile images in a shared database.

Hong et al propose that the constellation be extended to work in two modes, nominal and disaster. On the outset of a disaster, satellites would maneuver to lower orbits to provide higher resolution images of the area of interest. When the mission is complete, the satellites would return to their normal orbits and await the next command. Operating at the lower altitude exposes the satellites to greater atmospheric drag forces and, therefore, must eventually return to the higher orbit or be overcome by the drag. Additionally, maneuvering would consume considerable propellant, a mission for which the constellation is not currently designed. When satellites run low on propellant they are no longer able to perform station-keeping and are forced to de-orbit. However, the authors propose an on-orbit supply depot to refuel the satellites after propellant is

expended. Though this concept has not been adopted, it may one day find use with the DMC or other satellite systems.

2.4. DARPA SeeMe Concept

The Defense Advance Research Projects Agency (DARPA) has awarded phase one of a program called Space Enabled Effects for Military Engagements (SeeMe). Raytheon will assist DARPA in completing the design for a constellation of satellites that provide high resolution imagery from LEO more efficiently than is currently available. The request for proposal gave broad specifications that will be refined by DARPA and Raytheon in 2013. The envisioned constellation will contain approximately 24 satellites in low inclination circular orbits at an altitude between 200 km and 300 km. The lifespan of each satellite is expected to be between 30 days and 120 days and a mortality rate of 20% will be seen as acceptable. The overall objective of the program is to offer imagery direct to the user at NIIRS 5.5.

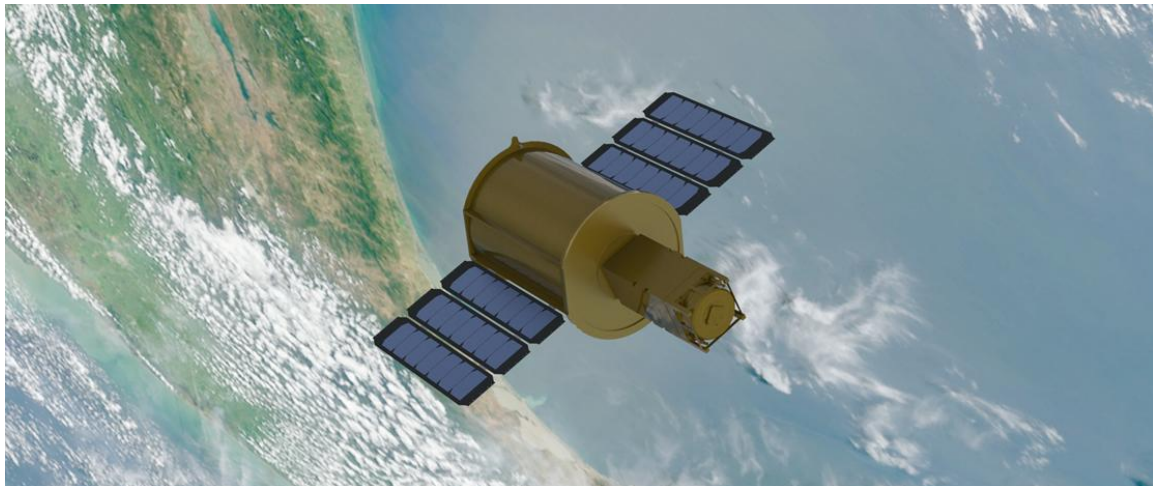


Figure 3. DARPA SeeMe Satellite (Artist's Concept)

SeeMe will attempt to merge “tactical effectiveness and economic efficiency” and seeks to compete at UAV-like costs. Unlike UAVs, the satellite constellation would be postured to support non-continuous operational tempos by being quickly deployable and relatively disposable. This differs from the mobilization required to deploy a squadron of UAVs to a remote theater of operations with the support required to carry out operations for an unknown period of time.

DARPA is in favor of using the Airborne Launch Assist Space Access (ALASA) platform for launch and orbit insertion. Although other options will also be considered, DARPA feels that ALASA will offer a truly responsive capability at a low cost. If successful, SeeMe will make on-demand imagery available to tactical troops in areas where UAV operations are not possible.

2.5. SMDC NanoEye Concept

The Army’s Space and Missile Defense Command (SMDC) is also developing a system to provide high-resolution imagery to the tactical level through their NanoEye system. The envisioned constellation consists of approximately 12 satellites in circular orbits at an altitude of 600 km. The distinguishing characteristic between NanoEye and SeeMe is the ability to maneuver. The 20 kg (dry-mass) NanoEye satellite will carry approximately 60 kg of propellant allowing for greater than 2.5 km/s second of ΔV . When high resolution imagery is required, individual satellites will maneuver to an eccentric orbit with perigee at 175 km (over the target) to achieve resolution of NIIRS level 6 at nadir.

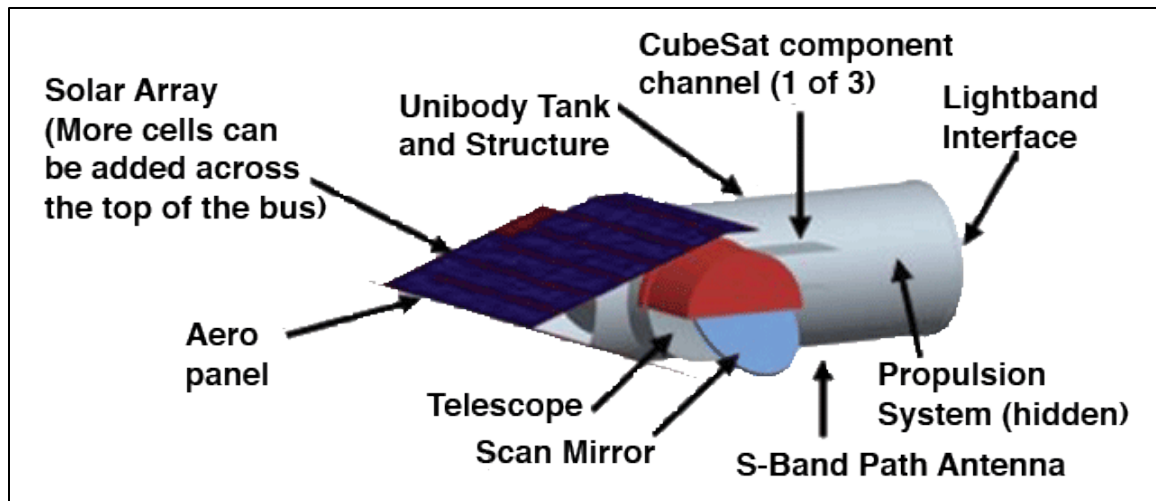


Figure 4. NanoEye sketch with Components Labeled

Each satellite is estimated to have a lifespan of up to three years, but maneuvering would quickly deplete the propellant limiting service life by the ability to perform stationkeeping. The original objective of the program was to produce a satellite with production and launch costs each of one million dollars. The exact cost of production will depend on the number of satellites produced. The most recent estimates from by the satellite designer are \$1.4M per unit. Launch costs are also variable, depending on the CONOPS, launch vehicle used, and number of launches.

SMDC's NanoEye could provide imagery to tactical level forces in response to developing situations in both conflict and natural disaster. The analysis in the following chapters centers on the feasibility of the NanoEye concept and explores methods of maximizing constellation coverage and investigating the consequences maneuvering will have on constellation management. Particular attention will be paid to the build-up phase of the proposed constellation.

2.6. Summary

The methods in the following chapter use this literature review as a foundation for examining a specific case. The choice of constellation is based upon the research of many great scientists mentioned in this chapter. The overall goal of my research is to determine feasibility of the NanoEye system; many factors must be considered before such a recommendation can be made. The topics discussed here will become considerations in examining a dynamic constellation.

III. Methodology

3.1. Introduction

This chapter gives a detailed description of the methodology used to explore the Space and Missile Defense Command (SMDC) NanoEye constellation concept and describes how to best approach this constellation in the build-up phase and during early operations. Several alternatives are compared in order to determine the most advantageous configuration to perform the NanoEye mission. Circular orbits will be examined first, followed by an analysis of eccentric orbits. The NanoEye concept proposes maneuvering satellites from 600 km circular orbits to eccentric orbits with apogee altitude at 600 km and perigee altitude at 175 km in response to user requests for high resolution imagery. Satellites operating in the eccentric orbit will experience a different set of forces and perturbations than those acting on satellites in the circular orbit. These perturbations will change the position and velocity of the satellites and the circular and eccentric orbits will diverge over time. Constellation management (stationkeeping) will be addressed in order to maintain the relative spacing of the planes of the orbits as well as the relative spacing of the satellites within these planes. The propellant required (ΔV) for constellation management will be quantified in order to make recommendations for or against the maneuvering concept of operations (CONOPS) proposed by SMDC. This chapter is meant to provide a repeatable method for calculating the stationkeeping requirements associated with maneuvering and a starting point for further research.

3.2. Orbit Selection

Using the specifications provided by SMDC on the NanoEye concept, the first major task to approach feasibility is to determine practical orbits and constellations for the NanoEye mission. Based on the research by Hanson, Middour, and Turner, the search begins with symmetric Walker constellations. The parameters of satellite altitude and eccentricity will be defined by the SMDC literature. The elevation angle will also not be altered as this is a characteristic of the satellite payload. The parameters left to define are inclination, number of satellites, number of planes, and phasing between the planes. It is necessary to briefly introduce some terminology from orbital mechanics to discuss the subject in more detail.

The classical orbital elements (COEs) will be used to describe the size, shape, and placement of a satellite's orbit. The COEs are semi-major axis (a), eccentricity (e), inclination (i), argument of perigee (w), right ascension of the ascending node (RAAN) (Ω), and true anomaly (v). For a complete description of the COEs, refer to *Spaceflight Dynamics* by Wiesel.

The NanoEye literature specifies that satellites will operate in two classes of orbits: circular and eccentric. The size, described by a , and shape, described by e , for these orbits are defined. In the circular orbit, the semi-major axis is the sum of the radius of the Earth (6378 km) and the orbit altitude. The eccentricity of a circular orbit is zero, by definition. The argument of perigee is not defined for a circular orbit. RAAN and inclination will be discussed in more detail in later sections.

The semi-major axis for the eccentric orbit is calculated using the formula:

$$a_{\text{eccentric}} = \frac{(r_a + r_p)}{2} \quad (2)$$

$$a_{\text{eccentric}} = \frac{(6978 \text{ km} + 6553 \text{ km})}{2}$$

$$a_{\text{eccentric}} = 6765.5 \text{ km}$$

The eccentricity of the orbit is calculated using the formula:

$$e = \left[\left(\frac{r_a}{r_p} \right) - \frac{1}{(r_a/r_p)} + 1 \right] \quad (3)$$

$$e = \left[\left(\frac{6978 \text{ km}}{6553 \text{ km}} \right) - \frac{1}{(6978 \text{ km}/6553 \text{ km})} + 1 \right]$$

$$e = 0.0314$$

The argument of perigee will be placed at the latitude coinciding with the target in order to maximize the image resolution.

The next COE discussed is inclination. The research of Wertz, Larrimore, and Sugrue suggest orbits with inclination slightly higher than the latitude of the target to maximize coverage. The target of intended surveillance is a location on the Earth defined by a latitude and longitude. To optimize coverage of this location, a low Earth orbit is selected with an inclination tuned to maximize the number of accesses of the target while minimizing the time between accesses. Sugrue has shown that the value for inclination that maximizes coverage of a target is determined by the formula:

$$i = \Phi_{\text{target}} + \lambda \quad (4)$$

where i is the inclination, Φ_{target} is the target's latitude, and λ is the Earth central angle.

The Earth central angle (λ) is determined by the formula:

$$\sin (\lambda + \varepsilon) = \frac{[R * \cos (\varepsilon)]}{[R + h]} \quad (5)$$

where ε is the minimum elevation angle, R is the radius of the Earth, and h is the orbit altitude.

The final two orbital elements to discuss are RAAN and true anomaly. For symmetric constellations with multiple orbital planes, the RAAN of each plane will be equally spaced around the Earth. Now that we have defined the size, shape, and placement of each orbit, it remains to determine the placement of the satellites within these orbits. For an orbital plane with multiple satellites, the true anomaly (v) of each satellite will be equally spaced around the orbit. The placement of satellites in one plane with respect to adjacent planes will be determined by the phasing parameter (F).

Turner's will be used to calculate the phasing parameter:

$$F = (P - 1) - (T / P)$$

where F is the phasing parameter, P is the number of planes, and T is the total number of satellites in the constellation.

This completes the discussion on orbits. To determine the inclination of the orbits, it is first necessary to determine the latitude of the target.

3.3. Target Selection

The target considered in this thesis is Dayton, Ohio. This location has been chosen arbitrarily and has a latitude of 39.7589° North and a longitude of 84.1917° West. Two possible scenarios requiring immediate surveillance are disaster relief efforts and combat operations. The justification for studying satellite surveillance in response to these situations is that these events may unfold quickly and occur in areas not accessible

by UAVs. Domestic regulations and airspace congestion may also prohibit the use of UAVs.

It is now possible to imagine a NanoEye satellite responding to a disaster and providing time critical surveillance of a target. Unfortunately, a LEO satellite can only provide short windows of access even when the orbit is optimized for coverage. Each NanoEye satellite can see a circular area with a radius of 1000 km at any given time (approximately 0.6% of the Earth's surface area). Therefore, a constellation of satellites must be deployed to provide a steady flow of information.

3.4. Constellation Design

This section discusses the analysis needed to design a constellation for NanoEye. The NanoEye literature does not specify the constellation or number of satellites for an operational system. Therefore, an assumption must be made to conduct a comparative analysis. It is assumed that six satellites are available for launch at the outset of an event and launch can occur individually, in pairs, triplets, or all together. Coverage will be calculated for a six satellite constellation in multiple configurations. The focus on a six satellite constellation does not imply an optimal solution. Adding additional satellites to the constellation will improve coverage metrics and system robustness, but six satellites is a reasonable starting point. Table 3 describes the four configurations that will be considered.

Table 3: Possible Constellations

# of Satellites	# of Planes	# of Satellites per Plane
6	1	6
6	2	3
6	3	2
6	6	1

Each constellation distributes the satellites evenly among their planes and all satellites are in circular orbits with the same inclination; they are all symmetric. These constellations will be compared to find the one with the most number of accesses and the least time between revisits.

The minimum elevation angle is set to 20° in accordance with the SMDC NanoEye literature. Additionally, both day and night passes will be considered in the STK coverage analysis. This is in contrast to Sugrue's MATLAB code which did not impose a minimum elevation angle between the satellite and the target but rather required a sun elevation angle of zero degrees or greater (daylight passes).

3.5. Coverage Geometry

This section describes the terms associated with coverage and also considers the inputs to coverage analysis. Satellite coverage depends on the altitude of the satellite as well as the minimum elevation angle and maximum slant range of the instrument(s). For circular orbits, the altitude is approximately constant throughout the orbit. Coverage tells us what we can see and how often we can see it. Field-of-view describes the area on the surface of the Earth that could be viewed by a satellite at any given time, based on the satellite's altitude. When we consider the limitations of the payload (elevation angle and

slant range), we describe the field-of-regard. Both the field of view and field of regard are ellipses centered at the point on the Earth's surface directly below the satellite. The field of view extends to the local horizon, whereas the field of regard covers a smaller area and accounts for obstructions to the line of sight. The Earth central angle (λ) is half of the angle of the cone in which the satellite's sensor can collect data, as seen in Figure 5. In the Dayton scenario, the field of regard will be limited by elevation angle (ϵ) but not by slant range. The equations to arrive at the Earth central angle are as follows:

$$\sin(\rho) = \frac{R_E}{R_E + H} \quad (6)$$

$$\sin(\eta_{max}) = \sin(\rho) * \cos(\epsilon_{min}) \quad (7)$$

$$\lambda_{max} = \frac{\pi}{2} - \epsilon_{min} - \eta_{max} \quad (8)$$

where ρ and η are the angles from the spacecraft to the local horizon and the limits within minimum elevation angle, respectively. A visual aid for the geometry described above is shown in the following figure.

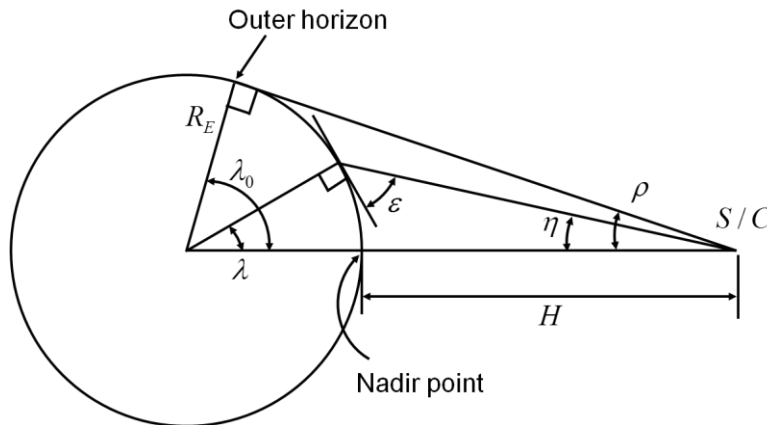


Figure 5. Angular Geometry for Spacecraft with Elevation Angle Constraint

This method for determining λ is equivalent to using Equation 5 but has the benefit of visualizing the orbital geometry. If the payload is also limited by a maximum slant range, a different set of equations determines the Earth central angle.

The diameter of the field of regard is called the swath width and contributes to a band of coverage that can be drawn as a ground track for a satellite pass, seen in the figure below.

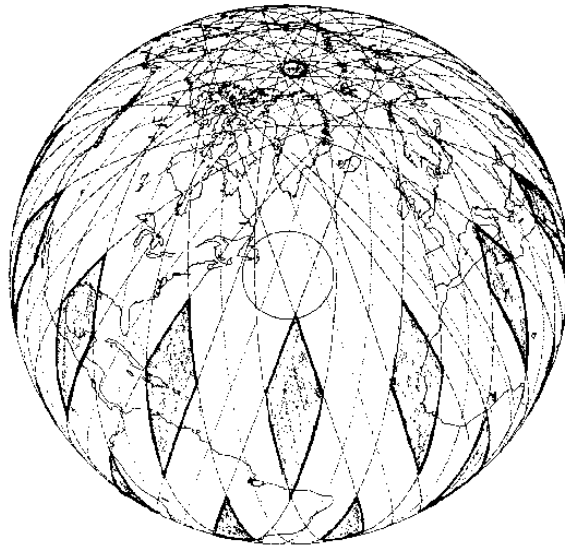


Figure 6. Swath Width and Ground Track Shown on Earth

The ground track has a westward shift due to the rotation of the Earth beneath the plane of the orbit. Depending on the period of the orbit and the swath width, the satellite may have access to the target on multiple subsequent orbits followed by a number of orbits that provide no access (see equations 3.10 through 3.11 in Sugrue for mathematical proof of number of successive passes).

3.6. Computer Simulation

Sugrue created an algorithm to numerically integrate the position of a satellite given a set of initial conditions. The state vector is defined as $X^T = [x \ y \ z \ \dot{x} \ \dot{y} \ \dot{z}]$ and the equations of motion are constructed to include the J_2 perturbation due to the oblateness of the Earth. Sugrue's algorithm also considers the Sun angle to determine if satellite coverage of the target occurred during daylight conditions. The output of the algorithm is the number of satellite accesses and the duration of each access as well as the time and date at which the access occurs. Additionally, slant range is recorded for each time step during an access where average and max slant range are recorded for analysis periods.

STK is also capable of providing coverage analysis. Propagation in STK can consider only the J_2 perturbation, but may also be used to examine the effects of higher order perturbations. Initially, only the J_2 perturbation will be considered in order to validate Sugrue's code. STK is able to output the number of accesses, coverage times, and range to the target during accesses. In addition to the parameters examined by Sugrue, STK will also be used to report the percent of time a constellation provides coverage of the target, the time average gap, and the maximum response time. STK defines time average gap as the average length of the coverage gap during the interval and maximum response time as the longest gap between coverages over the entire interval. The mathematical definition for the former is:

$$\text{Time Average Gap} = \frac{\sum(\text{Gap Duration})^2}{\text{Coverage Interval}} \quad (9)$$

After validating the two-body simulation against Sugrue's method, STK will propagate using the High-Precision Orbital Propagator (HPOP) to ensure inclusion of

atmospheric drag forces. Atmospheric drag cannot be included using the J_2 propagator in STK. Even when using the HPOP, atmospheric conditions are generalized and use average conditions throughout scenarios. Appendix A describes the steps necessary to accurately model atmospheric drag using a catalog of historical data. In this way, known periods of solar maximum and solar minimum conditions can be simulated to compare the effects of atmospheric expansion and increased drag on LEO satellites. This method of modeling the atmosphere significantly increases the computing time compared to the default settings but provides results that are much closer to realistic conditions.

Satellite operations under 200 km experience significant drag and are likely to re-enter the atmosphere within a period of weeks if energy is not added to compensate for the losses due to drag. Atmospheric drag is clearly important to consider when examining the NanoEye concept. Attention must also be paid to the other perturbations that tend to displace satellites in LEO. The coverage provided by a constellation is sensitive to the placement of the satellites within the constellation. If perturbing forces change the relative position of the satellites the coverage must be re-evaluated.

3.7. Perturbations

The perturbations caused by the non-circular shape of the Earth will cause the orbital plane to precess about the rotational axis of the Earth. This precession is a function of the orbit's semi-major axis, eccentricity, and inclination. Satellites in a constellation must match all three parameters in order to maintain the relative orientation of the orbital planes. With this in mind, it is clear that a satellite in an eccentric orbit will be affected differently by the perturbations than a satellite in a circular orbit.

The major disturbance in LEO is caused by the J_2 perturbation. Sugrue's thesis was limited to the J_2 perturbation on a single LEO satellite; however, it was recommended that future research include the force due to atmospheric drag as well as constellations. This thesis covers these two additional topics and also includes modeling of higher order spherical harmonics and third body effects.

3.8. Considerations for Eccentric Orbits

When individual satellites within the constellation maneuver into eccentric orbits, the perturbations from the oblateness of the Earth affect the orbit differently than the satellites in the 600 km circular orbit. Additionally, significant drag is experienced by the satellite as it descends to more dense atmospheric regions.

The RAAN will regress at a different rate in the eccentric orbit than in the circular orbit. This regression will cause the plane of the orbit to rotate away from the plane of the circular orbit, thereby separating the maneuvering satellite from the constellation even after the orbit is re-circularized. The equation for the regression of the node is given below from Wertz (*Mission Geometry*):

$$\frac{d}{dt}\Omega = \frac{-2.06474 \times 10^{14} * \cos i}{a^{7/2} * (1-e^2)^2} \quad (10)$$

The graph in Figure 7 shows the rate of RAAN regression as inclination is varied from zero degrees to 180°. RAAN regression is greatest for orbits with inclination near zero (equatorial orbits) and least for orbits with inclination near 90° (polar orbits).

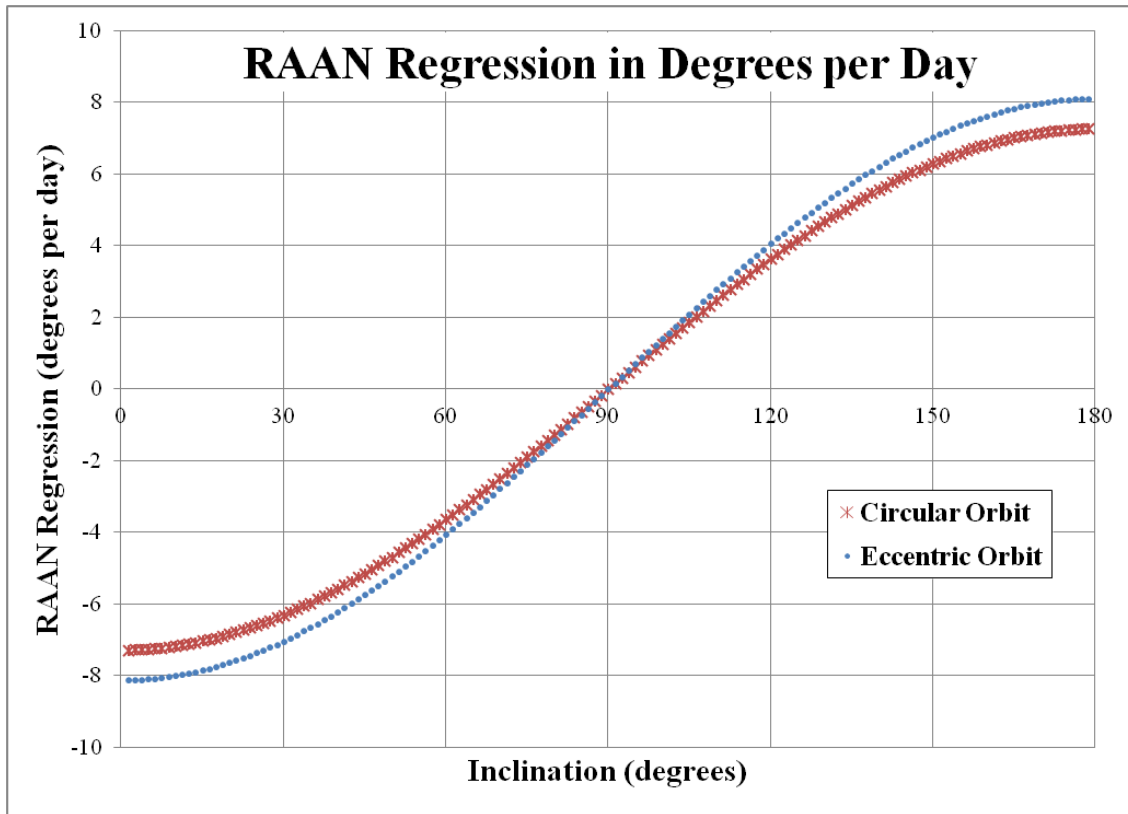


Figure 7: RAAN Regression vs. Inclination

A maneuver is commanded to increase image resolution and would therefore coordinate for perigee to occur directly over the target, to minimize the distance between the satellite and the target. The maximum resolution will occur at perigee looking nadir. Depending on the nature of the request, additional low altitude passes may be required. A satellite may maneuver into an eccentric orbit then re-circularize to return to the reference orbit and then maneuver again, completing two maneuver cycles to make two collections. On the other hand, the operator may choose to leave the satellite in the eccentric orbit until the next access in an attempt to save propellant. As the satellite maintains an eccentric orbit, the J_2 perturbation will cause the argument of perigee to

rotate in the plane of the orbit thereby placing perigee over a location away from the target on the next pass (see Figure 9). The equation from Sellers quantifies change per day in perigee rotation:

$$\frac{d}{dt} \omega = \frac{1.03237 \cdot 10^{14} \cdot (4 - 5 \sin^2 i)}{a^{7/2} \cdot (1 - e^2)^2} \quad (11)$$

The graph in Figure 8 shows the rate of perigee rotation as inclination is varied from zero degrees to 180°. Notice that perigee does not rotate for orbits with inclinations of 63.4° and 116.6°. This special inclination is used in Molniya Orbits for extended dwell times (apogee) over high latitudes in the Northern Hemisphere without a requirement for controlling the location of perigee.

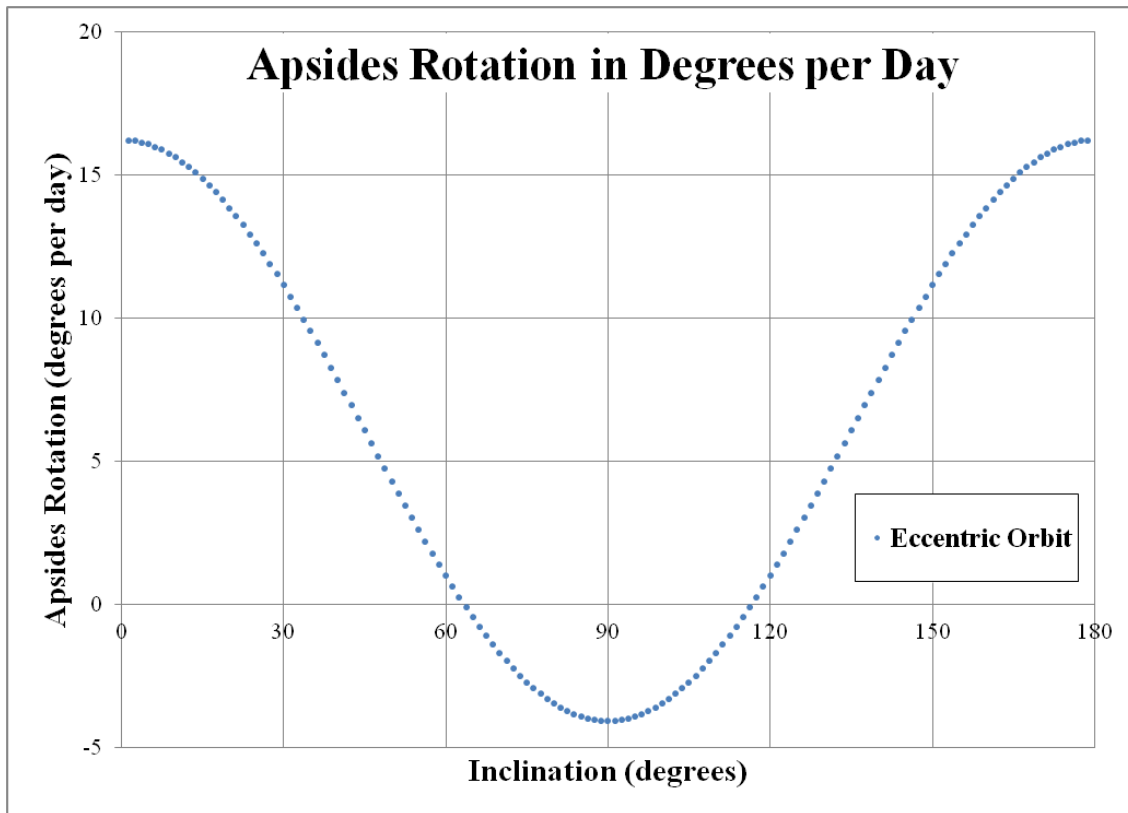


Figure 8. Apsides Rotation vs. Inclination

In addition to RAAN regression and perigee rotation, atmospheric drag will tend to decrease the semi-major axis and eccentricity of the orbit. The largest decrease in altitude will occur at apogee because the greatest drag force is experienced at perigee. If no compensation is made, the satellite will eventually re-enter the atmosphere. Clearly there are trade-offs between maneuvering for each individual collect and maintaining an eccentric orbit in preparation for subsequent taskings. Some analysis must be done to determine when the propellant required for stationkeeping exceeds the propellant required to perform major maneuvers.

Though the designers of NanoEye were not able to discuss the expected coefficient of drag (c_d) of the spacecraft, estimates can be made based on past satellites to get a reasonable approximation. A sensitivity analysis will be conducted to determine the possible errors associated with this unknown parameter.

The discussion above only addresses maintaining an orbit; position within the orbit must also be considered. As the satellite dips into the eccentric orbit, the period of the orbit decreases and the satellite completes more revolutions per time compared to the remaining satellites in the plane. Phasing maneuvers are required to reset the symmetry of the constellation. The amount of propellant required to conduct a phasing maneuver is inversely proportional to the time allocated for the maneuver. Vallado's method for Circular Coplanar Rendezvous is used to determine the ΔV required to return the satellite to its proper position within the circular orbit. The algorithm accounts for the number of orbits we allow the maneuver to occur within; this is equivalent to defining the time allowed for the maneuver. The algorithm begins by calculating the angular velocity of the target orbit.

$$w_{tgt} = \sqrt{\frac{\mu}{a_{tgt}^3}} \quad (12)$$

where μ is the gravitational constant and a_{tgt} is the semi-major axis of the target orbit.

The time allowed for the maneuver to complete is given by the formula below.

$$\tau_{phase} = \frac{2*\pi*k_{tgt}+\theta}{w_{tgt}} \quad (13)$$

where k_{tgt} is the number of orbits before rendezvous with the orbital position and theta is the required phase angle (the difference between the current and desired position within the orbit). The next parameter calculated is the semi-major axis of the phasing orbit.

$$a_{phase} = \left[\mu * \left(\frac{\tau_{phase}}{2*\pi*k_{int}} \right)^2 \right]^{1/3} \quad (14)$$

where k_{tgt} is the number of orbits the maneuvering satellite completes in the intermediate (phasing) orbit. The ΔV then is calculated using the formula:

$$\Delta V_{phasing} = 2 * \left| \sqrt{\frac{2*\mu}{a_{tgt}} - \frac{\mu}{a_{phase}}} - \sqrt{\frac{\mu}{a_{tgt}}} \right| \quad (15)$$

where the factor of two accounts for maneuvering into the phasing orbit and then re-circularizing the orbit after the satellite converges on the desired orbital position.

3.9. Evaluation Period

The period of evaluation is ten days. Surveillance of the target will be conducted by the constellation over this period of time. Coverage statistics will be determined, and are dependent on the position and spacing of the satellites within the constellation. The ten day period was chosen because rescue operations following a natural disaster and battlefield awareness in conflict are most critical in the first ten days. After ten days it is

assumed that operations will either become routine or other ISR assets will be deployed to provide a more persistent view of the region.

3.10. Summary

The methodology described in this chapter provides an opportunity to quantify the effects of perturbations on a maneuvering satellite. The propellant required to offset these perturbations is determined and listed in the results chapter. Coverage metrics will be determined for the baseline, six satellite, constellation as well as constellations in differing configurations.

IV. Analysis and Results

4.1. Introduction

This chapter presents the results of the analysis intended to validate the use of maneuvering LEO satellites to collect high resolution images for Earth surveillance. First, the optimal inclination will be determined to provide maximum coverage for a satellite with defined altitude, minimum elevation angle, and target latitude. Next, coverage characteristics will be examined for four different configurations of constellations, each containing six satellites in circular orbits. After a determination is made for the baseline constellation, analysis will be conducted to explore the implications of a satellite maneuvering and then returning to the constellation.

Maneuvering from a 600 km altitude circular orbit to an eccentric orbit with apogee at 600 km and perigee at 175 km will require a specific ΔV . Additionally, operating at a lower altitude will cause the satellite to experience a decrease in orbital period and an increase in atmospheric drag. Furthermore, operating in an eccentric orbit will cause the satellite to experience a change in the Right Ascension of the Ascending Node (RAAN) and the argument of perigee (w) due to the J_2 perturbation, as compared to the circular orbit.

The parameters above will be quantified and the ΔV that is required to maintain symmetry in the baseline constellation will be calculated. Expenditure of ΔV will decrease the operational life of the satellite.

4.2. Inclination

Sugrue has shown that to for maximum coverage of a target the inclination must be the summation of the target latitude and the Earth central angle of the spacecraft (see Figure 5). The Earth central angle of the spacecraft is a function of both altitude and minimum elevation angle. If a limit is set for slant range (distance to the target) then this parameter would also affect the Earth central angle. For the circular orbit with a constant altitude of 600 km and a minimum elevation angle of 20° , the Earth central angle is calculated using Equations 6 through 8 and has a value of 10.81° . The Earth central angle for a spacecraft at an altitude of 175 km and the same minimum elevation angle as above is 3.85° . When these angles are added to the target latitude, the optimal inclinations are 50.57° and 43.61° for the 600 km altitude pass and the 175 km altitude pass, respectively.

4.3. Coverage Analysis

Coverage analysis for circular orbits was the main topic covered by Sugrue in her 2007 thesis. STK modeling of two scenarios, originally analyzed using MATLAB by Sugrue, offers validation that the techniques for calculating coverage are roughly equivalent. For the following two scenarios the target latitude is set at 33° and a 30 day analysis period begins on 1 June 2004. The first case examines a satellite in a 350 km circular orbit inclined to 51° . Sugrue used an optimization technique to maximize the number of accesses over the analysis period. Using the same process described in Sugrue's thesis, the orbit that maximized coverage occurred at RAAN of 68° and true

anomaly of 90° . The coverage characteristics reported by Sugrue are listed below and compared to the STK simulation.

Table 4: Coverage Validation at 350 km

	Sugrue	STK	% Difference
Number of Daylight Passes	186	183	1.6%
Total Coverage Time (hours)	21.1	21.7	2.6%
Average Pass Length (minutes)	6.8	7.1	4.4%
Average Slant Range to Target (km)	1381	1568	13.5%
Maximum Slant Range to Target (km)	2102	2179	3.7%

With the exception of average slant range, all the values show a difference of less than five percent. Similarly, the second case models a satellite in an 850 km circular orbit inclined to 59° . The orbit that maximized coverage occurred at RAAN of 64° and true anomaly of 45° . The results are listed below.

Table 5: Coverage Validation at 850 km

	Sugrue	STK	% Difference
Number of Daylight Passes	204	192	5.9%
Total Coverage Time (hours)	39.2	44.0	12.2%
Average Pass Length (minutes)	11.5	13.7	19.4%
Average Slant Range to Target (km)	2101	2283	8.7%
Maximum Slant Range to Target (km)	3274	3320	1.4%

In this case, two values exceed a difference of ten percent, total coverage time and average pass length. In spite of the differences found between these two methods, Sugrue's MATLAB code and STK show general agreement. This validation of the

model was not intensely tuned but shows that the results are reasonable. The major apparent difference between the two methods is the model used for the Earth. The MATLAB model in Sugrue's thesis assumed a spherical model of the Earth whereas the model contained in STK is the World Geodetic System 1984 (WGS84) ellipsoid. STK does not offer any alternative Earth models to WGS84, so a more exact comparison was not possible. Though the Earth model likely accounts for the majority of the differences between the simulations, there may also be differences in the way the J_2 perturbations were propagated in Sugrue's code as compared to STK. Now that we have a baseline for calculating coverage from a single satellite we will next examine coverage provided by a constellation of satellites.

4.4. Constellation Coverage

Considering an initial constellation of six satellites, there are four possible symmetric constellation options as listed in Table 3. In each of these constellations, relative phasing of the satellites in adjacent planes must be considered in order to maximize coverage. Turner's formula (Equation 1) was used to determine the phasing parameter for the constellations.

Table 6: Phasing Parameters

# of Satellites	# of Planes	# of Satellites per Plane	Phasing Parameter
6	1	6	0
6	2	3	0
6	3	2	0
6	6	1	4

These four constellations were then modeled in STK with each satellite in a 600 km circular orbit inclined to 50.57° ($39.76^\circ + 10.81^\circ$), assuming that the first six NanoEye satellites will be launched into circular orbits and maneuvered into eccentric orbits on an as-needed basis. The following metrics were recorded: percent of time during the scenario that the target was visible by any satellite (both day and night); total number of accesses during the scenario; time average gap (Equation 9); and maximum response time. The values are listed below:

Table 7: Coverage for Circular Orbits Inclined to 50.57°

# Planes	# Satellites	% Time Covered	# of Accesses	Time Avg Gap (sec)	Max Response Time (sec)
1	6	8.72%	314	33306	55362
2	6	9.39%	323	4902	13437
3	6	9.23%	310	2658	5986
6	6	9.26%	319	3387	5771

Though all of the metrics should be considered when designing a constellation, the maximum response time is likely the most critical due to real-time information needs during contingency operations. The three plane and six plane constellations had comparable maximum response times, but the three plane configuration had a time average gap approximately 20% less than the six plane configuration. Both provided coverage for approximately 9.25% of the scenario time. The best constellation is the three plane configuration, based on the metrics in Table 7. As analysis shifts from the circular orbit to the eccentric orbit, only the three plane constellation will be examined.

Adding additional satellites should be considered if improved coverage metrics are desired and budgets allow.

4.5. Considerations for Eccentric Orbits

Maneuvering from a circular orbit to an eccentric orbit requires ΔV (propellant usage). Using the formulas for orbital velocity from Vallado, listed below, the ΔV can be determined for the maneuver between a 600 km circular orbit and an eccentric orbit with apogee altitude at 600 km and perigee altitude at 175 km.

$$v_{\text{circular}} = \sqrt{\frac{\mu}{r}} \quad (16)$$

$$v_{\text{eccentric}} = \sqrt{\frac{2\mu}{r} - \frac{\mu}{a}} \quad (17)$$

Approximately 0.1196 km/s ΔV is required to maneuver from a circular orbit to an eccentric orbit as described above. Therefore, the ΔV required to maneuver from a circular to an eccentric orbit and then return to a circular orbit would require 0.2393 km/s or approximately 239 m/s of ΔV . This excludes the additional ΔV required to overcome drag forces as well as the additional stationkeeping required to return to the assigned position within the constellation.

The perturbations caused by the equatorial bulge of the Earth, termed J_2 perturbations, will be the main cause of orbital drift for low Earth orbits. The eccentric orbit will precess at a different rate than the circular orbit, thereby separating the plane of the maneuvering satellite from the baseline constellation. The regression of the Right Ascension of the Ascending Node (RAAN) and the rotation of the argument of perigee will be solved analytically to include J_2 affects and will be compared to STK simulations.

Then, the STK propagator will be switched from J₂ to HPOP (including higher order perturbations and atmospheric affects) and the difference will be noted. The ΔV required to offset the orbital drift will be quantified and discussed in the sections that follow.

4.5.1. Node Regression and Perigee Rotation

The orbital plane of both the circular and eccentric orbit will experience a regression of the node due to the J₂ perturbation. Equation 10 approximates the regression of the node (from Wertz, *Mission Geometry*) and is used to find the precession of the orbital plane.

$$\frac{d}{dt}\Omega = \frac{-2.06474 \cdot 10^{14} \cdot \cos i}{a^{7/2} \cdot (1-e^2)^2}$$

$$\frac{d}{dt}\Omega_{\text{circular}} = -4.62^\circ \text{ per day}$$

$$\frac{d}{dt}\Omega_{\text{eccentric}} = -5.16^\circ \text{ per day}$$

$$\Delta \left[\frac{d}{dt}\Omega \right] = 0.538^\circ \text{ per day}$$

The differential regression of the RAAN between the circular and eccentric orbits due to J₂ is 0.538° per day.

An STK scenario was built to observe the differential regression of RAAN between a circular orbit and an eccentric orbit, using the J₂ perturbation propagator. Beginning 1 January 2014 with an initial RAAN of approximately zero degrees, after ten days the circular orbit's RAAN changed by 46.20° and the eccentric orbit's RAAN changed by 51.59°. Dividing the difference of these numbers by the number of days gives a differential regression of 0.539° per day, almost exactly the same rate given in the analytical method above. A sample of the STK output is included below. The report step

size of one day only reflects the sampling of the data and does not affect the calculations of the propagator.

Table 8: RAAN Regression with J_2 and Inclination 50.57°

<u>Time (UTCG)</u>	<u>Circular - RAAN (deg) [J_2]</u>	<u>Eccentric - RAAN (deg) [J_2]</u>
1/1/2014 16:00	359.89	359.89
1/2/2014 16:00	355.27	354.73
1/3/2014 16:00	350.65	349.57
1/4/2014 16:00	346.03	344.41
1/5/2014 16:00	341.41	339.26
1/6/2014 16:00	336.79	334.10
1/7/2014 16:00	332.17	328.94
1/8/2014 16:00	327.55	323.78
1/9/2014 16:00	322.93	318.62
1/10/2014 16:00	318.31	313.46
1/11/2014 16:00	313.69	308.30

The agreement between the analytical solution and the J_2 propagator in STK is very encouraging. Next, we can compare a more realistic simulation using the HPOP in STK.

Table 9: RAAN Regression with HPOP and Inclination 50.57°

<u>Time (UTCG)</u>	<u>Circular - RAAN (deg)</u> <u>[HPOP]</u>	<u>Eccentric - RAAN (deg)</u> <u>[HPOP]</u>
1/1/2014 16:00	359.89	359.89
1/2/2014 16:00	355.23	354.74
1/3/2014 16:00	350.59	349.49
1/4/2014 16:00	345.97	344.30
1/5/2014 16:00	341.36	339.13
1/6/2014 16:00	336.73	333.85
1/7/2014 16:00	332.08	328.66
1/8/2014 16:00	327.42	323.40
1/9/2014 16:00	322.77	318.14
1/10/2014 16:00	318.13	312.87
1/11/2014 16:00	313.51	307.60

The scenario shows a differential regression of the RAAN to be 0.591° per day which is within ten percent of the solution determined when only the J_2 perturbation was considered. Vallado states that J_2 dominates the other perturbations, the results above agree.

Next, we can quantify the amount of propellant necessary to compensate for the differential regression of the RAAN. The differential regression rate can be inserted in Vallado's algorithm (Equations 18 and 19) to determine the ΔV per day required to place the eccentric orbit back in the plane of the circular orbit. This ΔV must then be added as a stationkeeping requirement to return the orbital plane of the maneuvering satellite to its position in the constellation. Vallado's algorithm to determine ΔV_Ω for a circular orbit is as follows:

$$\Delta V_\Omega = 2 * v * \sin \frac{\vartheta}{2} \quad (18)$$

where ϑ is the angle defined by the equation:

$$\vartheta = \cos^{-1}[\cos^2(i) + \sin^2(i) * \cos(\Delta\Omega)] \quad (19)$$

Then, the ΔV_{Ω} is calculated for $\Delta\Omega$ of 0.591° is:

$$\Delta V_{\Omega} = 0.0602 \frac{\text{km}}{\text{s}} \text{ per day} = 60.2 \frac{\text{m}}{\text{s}} \text{ per day}$$

The symmetry of the constellation affects the coverage metrics. The following two tables compare the coverage metrics for the three plane, six satellite constellation after a ten day period in which one satellite per plane has operated continuously in the eccentric orbit and the RAAN has drifted by 5.91° . The constellations are otherwise symmetric. Table 10 shows coverage for the constellation where all satellites have maneuvered to the eccentric orbits.

Table 10: Coverage for Eccentric Orbits at Inclination 50.57° (RAAN Drift, Symmetric)

# Planes	# Satellites	% Time Covered	# of Accesses	Time Avg Gap (sec)	Max Response Time (sec)
Constellation with RAAN Drift (one satellite per plane; drift of 5.91 degrees)					
3	6	1.87%	122	13892	20251
Symmetric Constellation					
3	6	1.89%	122	13884	20117

In the eccentric orbit constellation, the coverage metrics are not significantly affected. Table 11 compares the constellation with one satellite per plane drifted 5.91° to the symmetric constellation. Now, all orbits are circular.

Table 11: Coverage for Circular Orbits at Inclination 50.57° (RAAN Drift, Symmetric)

# Planes	# Satellites	% Time Covered	# of Accesses	Time Avg Gap (sec)	Max Response Time (sec)
Constellation with RAAN Drift (one satellite per plane; drift of 5.91 degrees)					
3	6	9.28%	313	2664	8989
Symmetric Constellation					
3	6	9.23%	310	2658	5986

While metrics of coverage time and number of accesses slightly increase, there is a drastic increase (negative effect) in the maximum response time. In the worst case, the response time is increased by over 50%.

Just as the J_2 perturbation caused a regression of the RAAN, it will also tend to rotate an eccentric orbit within its orbital plane. When a satellite maneuvers to place perigee over the target, the argument of perigee immediately begins to rotate in the plane of the orbit. This effect is exaggerated in the following figure.

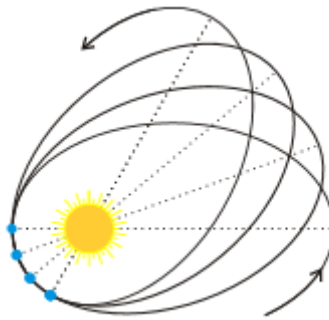


Figure 9: Apsides Rotation (Exaggerated)

If the operators of the satellite desire to keep the eccentric orbit then they would also require that perigee remain over the target latitude to enable collection of images

with the highest possible resolution. The equation to approximate the perigee rotation from Sellers is used (Equation 11).

$$\frac{d}{dt} \omega = \frac{1.03237 * 10^{14} * (4 - 5 * \sin^2 i)}{a^{7/2} * (1 - e^2)^2}$$

$$\frac{d}{dt} \omega = 4.13^\circ \text{ per day}$$

An STK scenario was built to observe the rotation of the argument of perigee with the J_2 perturbation propagator.

Table 12: Perigee Rotation with J_2 and Inclination 50.57°

Time (UTCG)	Arg of Perigee (deg) [J2]
1/1/2014 16:00	359.90
1/2/2014 16:00	4.03
1/3/2014 16:00	8.16
1/4/2014 16:00	12.29
1/5/2014 16:00	16.42
1/6/2014 16:00	20.55
1/7/2014 16:00	24.68
1/8/2014 16:00	28.81
1/9/2014 16:00	32.93
1/10/2014 16:00	37.06
1/11/2014 16:00	41.19

Beginning 1 January 2014 with an initial argument of perigee of approximately zero degrees, after ten days the Argument of Perigee had rotated 41.296° . Dividing by the number of days, this gives 4.13° per day, the same rate given in the analytical method above. The scenario then was modeled in STK using HPOP to predict the rotation of the argument of perigee, now accounting for higher order perturbations and atmospheric drag.

Table 13: Perigee Rotation with HPOP and Inclination 50.57°

Time (UTCG)	Arg of Perigee (deg) [HPOP]
1/1/2014 16:00	359.90
1/2/2014 16:00	3.62
1/3/2014 16:00	7.58
1/4/2014 16:00	11.46
1/5/2014 16:00	16.14
1/6/2014 16:00	20.75
1/7/2014 16:00	25.05
1/8/2014 16:00	30.25
1/9/2014 16:00	34.45
1/10/2014 16:00	36.64
1/11/2014 16:00	40.59

The perigee rotation over the ten day scenario was 40.691° with an average rate of 4.07° of rotation per day. The difference between the J₂ analysis and the HPOP analysis is less than two percent.

This rotation can be offset using an in-plane maneuver called an Apsides Burn. Applying ΔV at the common point between the current and desired orbit is possible such that only the argument of perigee (w) is affected and the semi-major axis and eccentricity remain unchanged. The equation by Sidi gives:

$$\Delta V_w = 2 \sqrt{\frac{\mu}{a*(1-e^2)}} e * \sin\left(\frac{\Delta w}{2}\right) \quad (20)$$

$$\Delta V_w = 0.0171 \frac{\text{km}}{\text{s}} \text{ per day} = 17.1 \frac{\text{m}}{\text{s}} \text{ per day}$$

The ΔV requirement is 17.1 m/s per day to maintain perigee over the target latitude.

If an apsides burn is not executed, perigee rotation will cause the location of perigee to rotate in the plane of the orbit at a rate of 4.1° per day at 50.57° inclination and 6.5° per day at 43.61° inclination. This does not significantly degrade coverage metrics

after a single orbit, but over the course of a few days will place perigee over a location that is of no interest to the user and increase the altitude of the satellite as it passes over the target, reducing the image resolution. The equation that relates radius (r) to true anomaly (v) is taken from Wiesel's text.

$$r = \frac{a(1-e^2)}{1+e*\cos(v)} \quad (21)$$

Now the satellite's altitude over the target can be determined as perigee rotates away from the target latitude. Altitude over the target latitude is listed for both 50.57° and 43.61° inclination in the tables below.

Table 14: Altitude Over Target Latitude as a Function of True Anomaly (v) at Inclination

50.57°

	v (degrees)	r (km)	alt (km)
	0.0	6553	175
After 1 Day	4.1	6554	176
After 2 Days	8.1	6555	177
After 3 Days	12.2	6558	180
After 4 Days	16.3	6561	183
After 5 Days	20.3	6566	188
After 6 Days	24.4	6571	193
After 7 Days	28.5	6577	199
After 8 Days	32.6	6585	207
After 9 Days	36.6	6593	215
After 10 Days	40.7	6602	224

Altitude over the target increases only one kilometer per day for the first two days and then increases at nine kilometers per day by the tenth day of uncontrolled perigee rotation.

4.5.2. Atmospheric Drag

A satellite in a 600 km circular orbit experiences very little atmospheric drag and would likely orbit unaided for many years before reentering. However, when the spacecraft's perigee altitude is reduced to 175 km, significant drag is experienced. Drag forces change with atmospheric conditions, are sensitive to solar conditions, and increase with atmospheric expansion during periods of intense solar activity. STK was used to model drag on the spacecraft during periods of solar extremes. 30 March through 9 April 2001 was chosen as the period to demonstrate the effects of solar maximum. Two other periods in 2003 were also modeled to examine the effects of extreme solar activity, the Halloween Storms of 2003. NASA states that "some of the most powerful solar storms ever recorded" occurred during this time period (Layton). Finally, 30 March through 9 April 2009 was chosen as the period to demonstrate the effects of solar minimum conditions. Each of the scenarios lasted ten days and updated the atmospheric model every three hours using Kp (planetary index measuring solar flux) values as inputs to the MSIS 2000 model. The MSIS 2000 atmospheric model, developed by the Naval Research Lab, was chosen and is extremely accurate for altitudes of zero to 1000 km. The mass of the satellite was set to 50 kg (to simulate propellant tank half-full) and the area to mass ratio was calculated to be $0.0042 \text{ m}^2/\text{kg}$. The coefficient of drag of NanoEye is unpublished but was estimated to be between 1.8 and 2.2 for the simulations. Appendix A further describes the methodology for configuring STK to model the atmosphere. Table 15 shows the minimum apogee altitude at the end of the ten day period for each simulation.

Table 15: Apogee Altitude for Inclination 50.57°

Start	Stop	Minimum Apogee Altitude (km)		
(mm/dd/yy hh:mm)	(mm/dd/yy hh:mm)	$c_d = 1.8$	$c_d = 2.0$	$c_d = 2.2$
3/30/2001 16:00	4/9/2001 16:00	474.7	460.5	445.6
10/25/2003 16:00	11/4/2003 16:00	484.3	471.6	458.3
11/1/2003 16:00	11/11/2003 16:00	503.7	494.0	483.0
3/30/2009 16:00	4/9/2009 16:00	529.2	523.0	516.6

The results show that the highest atmospheric drag forces were experienced during the March 2001 scenario followed by the October 2003 scenario. Solar maximum conditions degraded apogee altitude by more than 75% compared to solar minimum conditions. Examining a range of c_d values provides a sensitivity analysis for this parameter. Comparing the minimum apogee in each of the scenarios for c_d of 2.2 versus c_d of 1.8 gives a percent difference of around 20%. This gives us confidence that the range of possible drag forces is reasonably narrow even with uncertainty in c_d .

Figure 10 shows apogee versus time for a 30 day period to demonstrate the collapse of the eccentric orbit compared to the circular orbit.

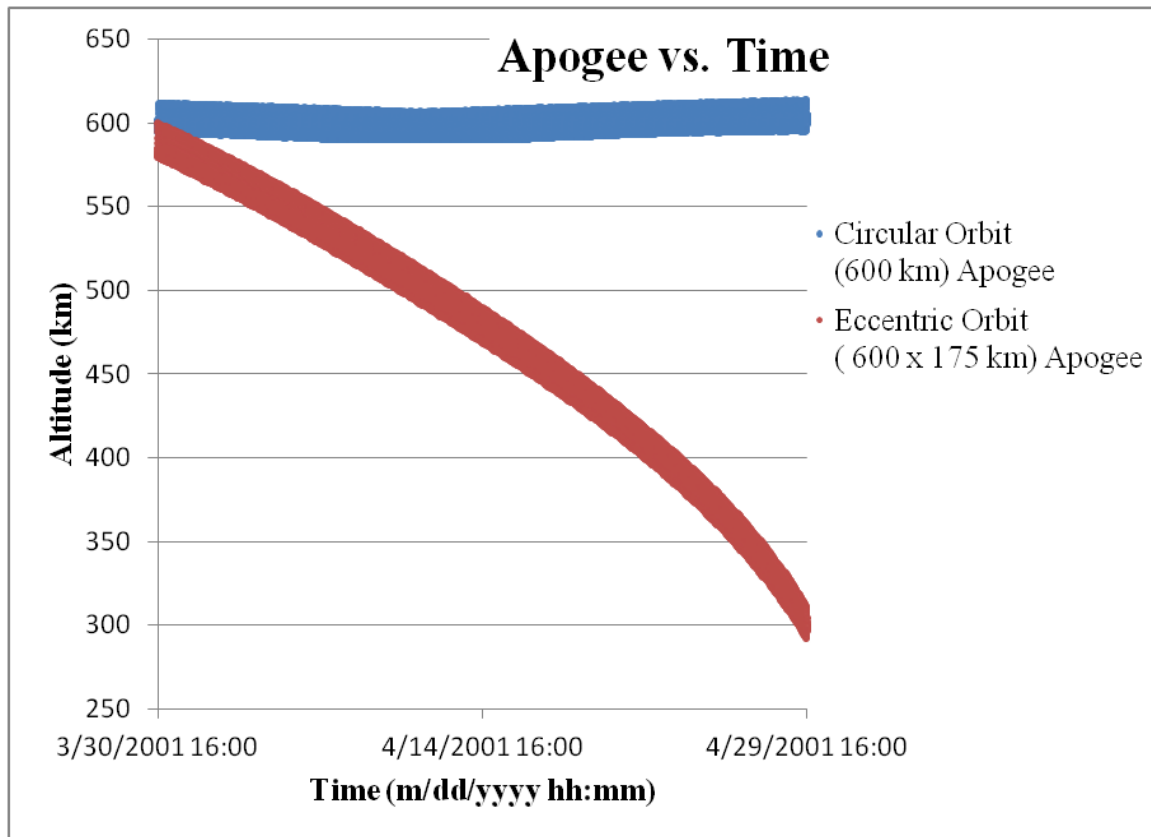


Figure 10: Apogee Altitude vs. Time for Circular and Eccentric Orbits

The width of the eccentric orbit's apogee altitude is shown in more detail in Figure 11. Apogee altitude is generally decreasing as seen in Figure 10 but oscillates around a decreasing mean value as time progresses. STK measures the distance in the nadir direction to the terrain which fluctuates as the satellite passes over terrain features. For the data in Table 15 and Table 25, the minimum value of apogee was retrained. As seen in the following plot, the last recorded value of apogee is not necessarily the minimum value during the scenario, possibly leading to incorrect conclusions. Therefore, retaining the minimum value clears up any ambiguity in this analysis.

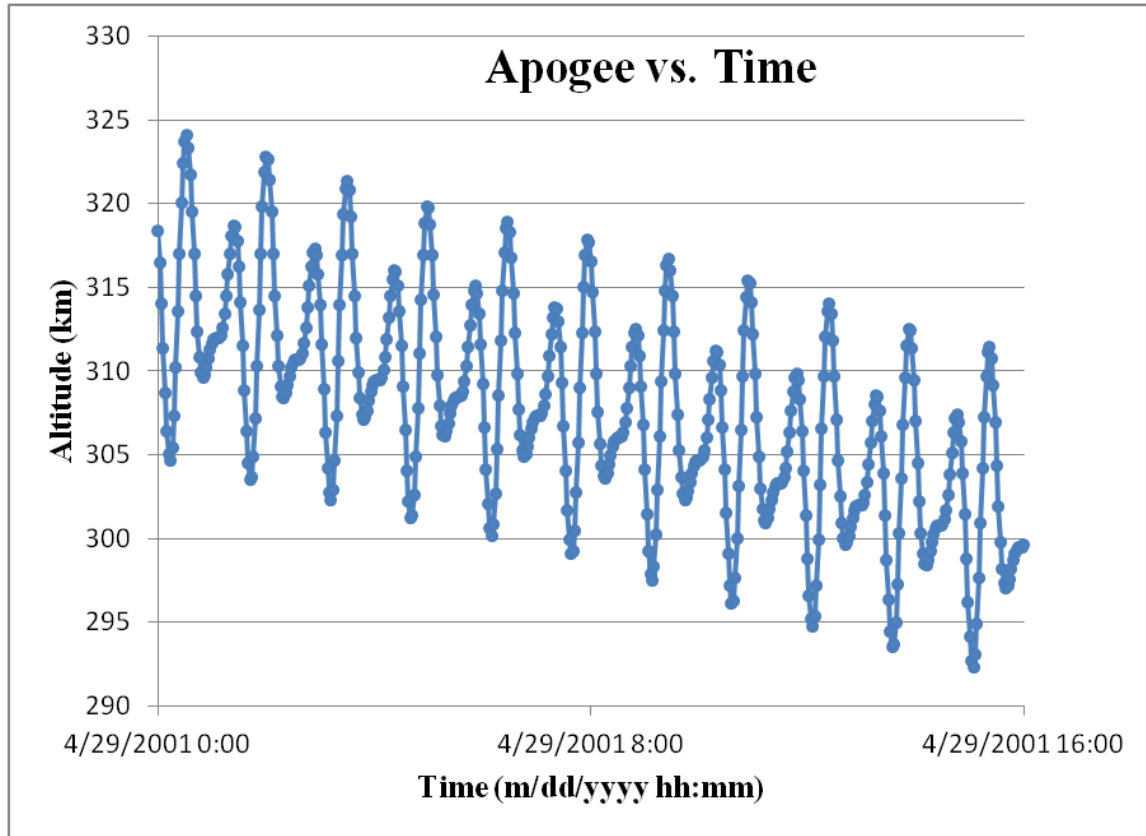


Figure 11: Apogee vs. Time (Showing Detail)

The apogee versus time plot is not a linear relationship but can be approximated as one for a ten day period. Based on the the values in Table 15, the apogee altitude is likely to decrease by between 71 km and 154 km in a ten day period. Using Equation 17, the required ΔV to regain these altitude losses are 0.0196 km/s and 0.0429 km/s (1.96 m/s and 4.29 m/s per day), for solar minimum and solar maximum respectively.

4.6. Phasing Maneuver

During the low altitude dip, the satellite advances in mean anomaly approximately 17° per orbit compared to the circular orbit. Raising the orbit above 600 km altitude will

allow the satellite to experience a greater orbital period and, therefore, fall back into the orbital position it left at the outset. Quantifying the ΔV required for this maneuver depends on time allowed for the maneuver to complete. The circular rendezvous maneuver is used to place the satellite back in its original orbit. A satellite orbiting at a constant 600 km circles the Earth approximately 15 times per day. Assuming that a satellite has access to the target for approximately three orbits per day, let us allow 12 orbits for the satellite to complete the phasing maneuver and return to its assigned orbital position before the next pass over the target.

If the satellite maneuvers into the eccentric orbit for three orbits it will advance approximately 51° compared to its position in the circular orbit. The values below show the process of determining the ΔV required for a 17° phasing maneuver in 12 orbits (using Equations 12-15).

$$w_{\text{tgt}} = 0.001083 \frac{\text{rad}}{\text{s}}$$

$$\tau_{\text{phase}} = 69887 \text{ s}$$

$$a_{\text{phase}} = 6996 \text{ km}$$

$$\Delta V_{\text{phasing}} = 0.020 \frac{\text{km}}{\text{s}} = 20.0 \frac{\text{m}}{\text{s}}$$

The following table performs the same series of calculations for 50° , 90° , and 180° . After completing a dipping maneuver over multiple days, a satellite may have a phase angle difference between zero degrees (best case) and 180° (worst case). A 90° phase difference will be considered an average phase difference for a multi-day maneuver.

Table 16: ΔV Required for Phasing Maneuver

Phase Angle	w_{tgt} (ras/s)	k_{tgt}	k_{init}	τ_{phase} (s)	a_{phase} (km)	ΔV_{init} (km/s)	ΔV (km/s)
17°	0.0010831	12	12	69887	6996	0.00988	0.020
51°	0.0010831	12	12	70435	7033	0.02940	0.059
90°	0.0010831	12	12	71063	7075	0.05142	0.103
180°	0.0010831	12	12	72513	7171	0.10078	0.202

4.7. ΔV Budgets for Maneuvering

The perturbations and atmospheric drag cause the maneuvering satellite to drift away from the initial orbit. If the constellation is to be maintained then propellant must be expended to overcome these differences. Let us call this special stationkeeping. If we total up the daily required special stationkeeping in Table 17 we see that a minimum of 79.3 m/s must be expended during solar minimum conditions to maintain the plane, placement of perigee, and apogee altitude during dipping.

Table 17: Daily ΔV Budget for Inclination 50.57°

	Solar Min	Solar Max
	(m/s)	(m/s)
RAAN Regression	60.2	60.2
Perigee Rotation	17.1	17.1
Atm Losses	2.0	4.3
<u>Daily Total</u>	<u>79.3</u>	<u>81.6</u>

This daily total can be added incrementally to the 239 m/s required to maneuver into the eccentric orbit and back to the reference circular orbit and the 103 m/s required to rephrase the orbit, as seen below.

Table 18: Running ΔV Total for 10 Days at Inclination 50.57°

	Solar Min	Solar Max
	(m/s)	(m/s)
After 1 Day	421	424
After 2 Days	501	505
After 3 Days	580	587
After 4 Days	659	668
After 5 Days	738	750
After 6 Days	818	832
After 7 Days	897	913
After 8 Days	976	995
After 9 Days	1055	1076
After 10 Days	1135	1158

In order to maintain perigee over the target for ten days and then return the satellite to the appropriate orbit requires 1135 m/s ΔV during solar minimum conditions. For extreme solar conditions like March 2001, a daily total for special stationkeeping is 81.6 m/s and over a ten day period requires 1158 m/s ΔV for a satellite to return to the circular orbit in the constellation. These totals are within the 2.5 km/s ΔV budget that the NanoEye developers advertise, but are still very expensive.

The procedure outlined above describes maneuvering to counter all of the perturbing forces that act on the satellite while in the eccentric orbit. Perhaps other operating concepts allow for acceptable coverage without countering all of the perturbations. For example, if we allow the RAAN of the orbit to drift but freeze the position of perigee over the target and compensate for atmospheric losses, then the daily ΔV budget is 19.1 m/s versus the previous 79.3 m/s. Using this assumption, the maneuvering satellite leaves the plane of the circular orbit and constellation management

is not maintained, but more propellant is conserved. A new ten day ΔV budget looks like:

Table 19: Running ΔV Total for 10 Days at Inclination 50.57° (RAAN Drift)

	Solar Min	Solar Max
	(m/s)	(m/s)
After 1 Day	361	363
After 2 Days	380	385
After 3 Days	399	406
After 4 Days	418	428
After 5 Days	437	449
After 6 Days	456	470
After 7 Days	475	492
After 8 Days	494	513
After 9 Days	514	535
After 10 Days	533	556

If a great number of satellites exist in the fielded NanoEye system, constellation management may be less of a concern. Sauter’s discussion of asymmetry through pseudo-random satellite placement could be used in conjunction with “coverage gap filling” to achieve acceptable coverage metrics. However, in the six satellite constellation, the coverage is significantly degraded as the satellites’ planes drift away from the reference constellation. If one satellite in each plane is allowed to drift over a period of ten days (5.91°) the maximum response time is increased by over 50% (see Table 11).

Another situation that avoids the requirement to correct the RAAN is when all six satellites perform the dipping maneuver together. In this case, the perturbing forces act

uniformly on the entire constellation. The constellation could survive for over 100 days in the eccentric orbits if only perigee location and apogee altitude are corrected.

A contrasting alternative to the CONOPs above is to maneuver into the eccentric orbit ‘on demand’ for an individual orbit rather than for an extended period of time. For each commanded maneuver, the ΔV cost would be 239 m/s to dip perigee and then re-circularize, in addition to the special stationkeeping required to offset the perturbations experienced during the maneuver. Rather than look at recovering the change per day in RAAN, perigee rotation, and apogee altitude, it is appropriate to quantify these changes per orbit.

The period of the eccentric orbit can be calculated using the following equation:

$$\text{Period} = 2\pi \sqrt{\frac{a^3}{\mu}} \quad (21)$$

Equation 21 yields a value of 5538 seconds, or 0.0641 days, for the eccentric orbit. The ΔV required per orbit is shown in Table 20.

Table 20: ΔV Budget per Orbit for Inclination 50.57°

	Solar Min	Solar Max
	(m/s)	(m/s)
RAAN Regression	3.9	3.9
Perigee Rotation	1.1	1.1
Atm Losses	0.1	0.3
Phasing Maneuver	20.0	20.0
<u>Orbit Total</u>	<u>25.1</u>	<u>25.2</u>

The addition of the maneuver itself (239 m/s) and the special stationkeeping (25.1 m/s) increases the total ΔV required for low altitude collects to 264 m/s per orbit, thus

returning the satellite to the circular orbit with proper spacing in the symmetric constellation. If the location of perigee is allowed to drift during a single orbit, the ΔV requirement drops to 24 m/s per orbit. Considering the ΔV budget required for a single orbit maneuver, a NanoEye satellite could perform up to nine maneuver cycles within the 2.5 km/s ΔV budget.

4.8. Revisiting Inclination

The assumption made for inclination was based on maximizing coverage for the constellation at 600 km. If the majority of a satellite's operations will be conducted at 600 km, the inclination should be set to 50.57° . If a satellite will be launched in direct response to a disaster and the majority of the operations will be conducted in the eccentric orbit, it may be prudent to match the orbit's inclination to the lower altitude in order to maximize coverage. When imaging passes are made at 175 km the field of view is appreciably decreased and the Earth central angle must be reevaluated. The Earth central angle of a satellite at 175 km altitude is 3.85° which agrees with the estimates published in the NanoEye literature, "2-4 degrees higher than the latitude of interest." The optimized inclination for the eccentric orbit is 43.61° . The table below compares the coverage characteristics for the four combinations of inclination and operating altitudes.

Table 21: Coverage for Circular and Eccentric Orbits at Inclinations 50.57° and 43.61°

# Planes	# Satellites	% Time Covered	# of Accesses	Time Avg Gap (sec)	Max Response Time (sec)
Inclined to 50.57 degrees, operating in circular orbits					
3	6	9.23%	310	2658	5986
Inclined to 50.57 degrees, operating in eccentric orbits					
3	6	1.89%	122	13884	20177
Inclined to 43.61 degrees, operating in circular orbits					
3	6	10.49%	279	2561	4376
Inclined to 43.61 degrees, operating in eccentric orbits					
3	6	3.14%	226	5001	10122

Matching the 43.61° orbit with operations conducted in the eccentric orbit provide almost a 100% improvement in number of accesses, time average gap, and maximum response time. The decrease in coverage metrics for the circular orbit operating at the non-optimal inclination only degrades the number of accesses by about ten percent and actually increases the other metrics of interest. A decision must be made whether to optimize operations for the circular orbit, the eccentric orbit, or to find a reasonable compromise in between. Figure 12 and Figure 13 show the distribution of accesses based on minimum slant range to the target during each access. For the range to be less than 200 km the ground track must nearly intersect the target exactly; the accesses with slant ranges greater than 600 km occur during passes where the ground track is hundreds of kilometers from the target. In both cases perigee is maintained over the target latitude. Figure 12 show the accesses for 50.57° and Figure 13 shows the accesses for 43.61°.

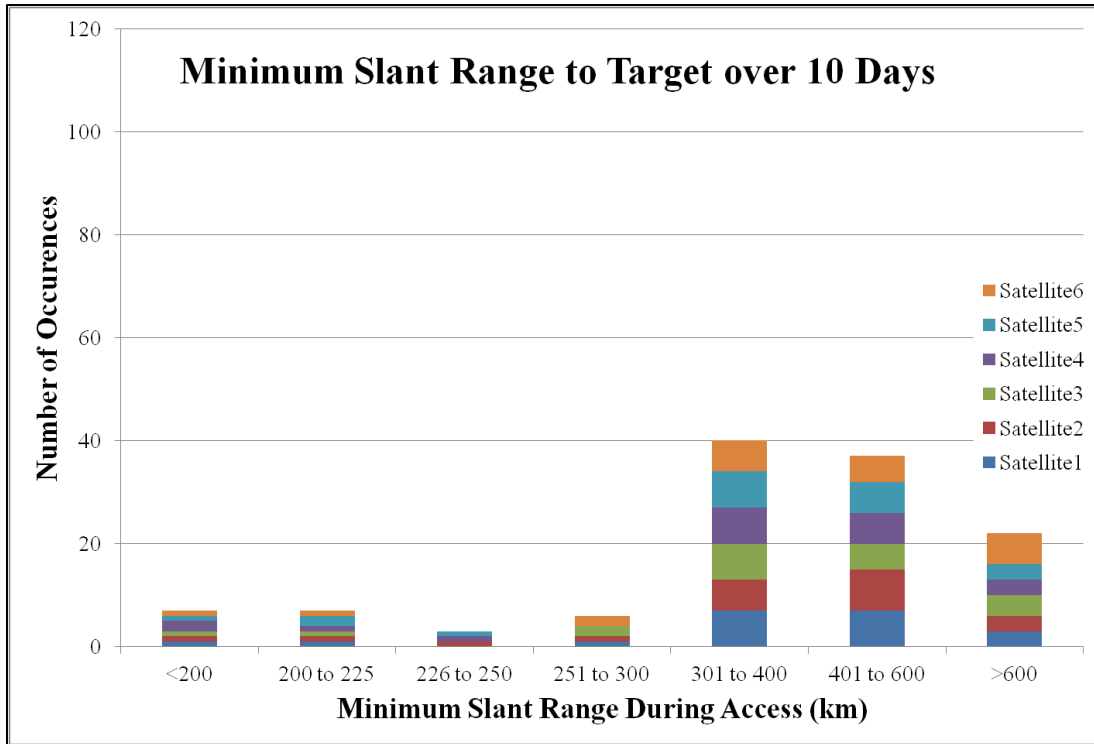


Figure 12: Slant Range Histogram for Eccentric Orbits at 50.57° Inclination

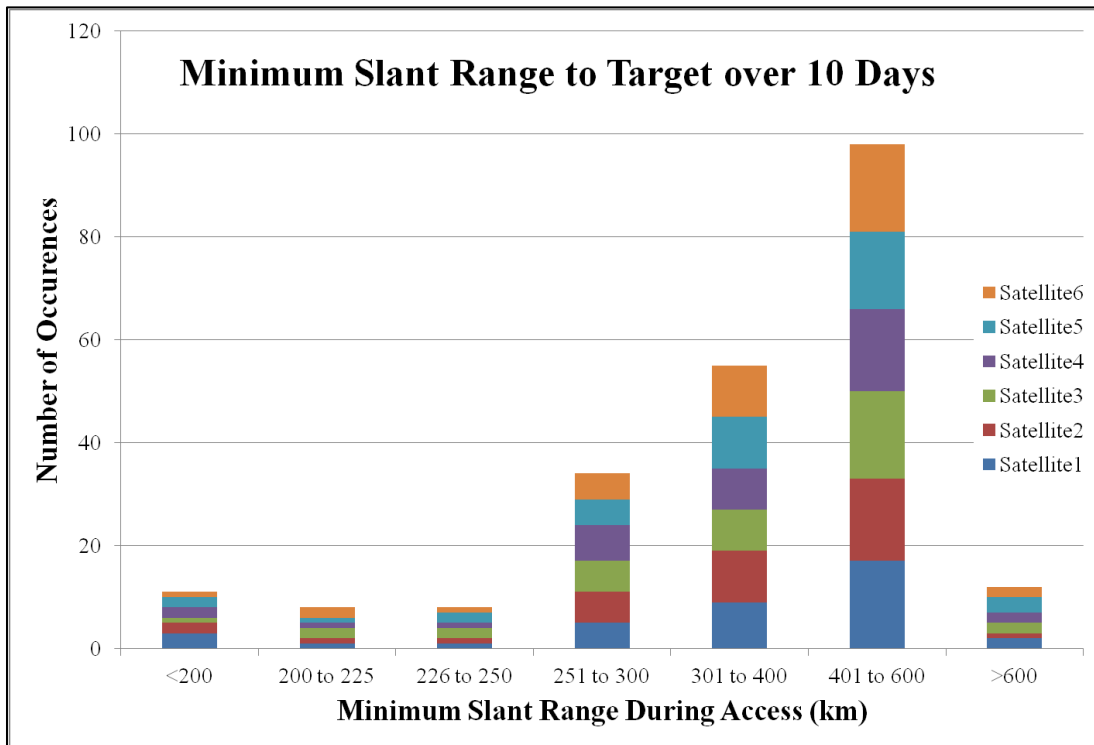


Figure 13: Slant Range Histogram for Eccentric Orbits at 43.61° Inclination

The slant ranges from circular orbits are all at least 600 km. The tables of data associated with Figure 12 and Figure 13 can be found in Appendix C (Table 38 and Table 39).

If the user chooses a particular inclination and wishes to change to the other, a plane change maneuver can be performed. Vallado's formula quantifies the ΔV required for a maneuver between 50.57° and 43.61° inclination at 600 km altitude.

$$\Delta V_i = 2 * v * \sin\left(\frac{\Delta i}{2}\right) \quad (22)$$

$$\Delta V_i = 0.9175 \frac{\text{km}}{\text{s}} = 918 \frac{\text{m}}{\text{s}}$$

Such a maneuver would significantly deplete the satellite's ΔV .

All of the analysis conducted for perturbations and ΔV budgets at an inclination of 50.57° will be repeated for orbits inclined to 43.61° . The differences shown for coverage and ΔV budgets for each inclination should help users determine a constellation that matches their particular needs. Using Equations 10 and 11, the difference in the regression of the RAAN is 0.6135° per day and the perigee rotation is 6.584° per day. Both of these values are greater than the perturbations observed in the orbit inclined to 50.57° . STK was simulated using the HPOP to estimate the differential RAAN drift, accounting for J_2 and higher order perturbations as well as atmospheric drag.

Table 22: RAAN Regression with HPOP and Inclination 43.61°

<u>Time (UTCG)</u>	<u>Circular - RAAN (deg)</u> <u>[HPOP]</u>	<u>Eccentric - RAAN (deg)</u> <u>[HPOP]</u>
1/1/2014 16:00	359.91	359.90
1/2/2014 16:00	354.60	354.02
1/3/2014 16:00	349.30	348.04
1/4/2014 16:00	344.03	342.13
1/5/2014 16:00	338.76	336.21
1/6/2014 16:00	333.49	330.19
1/7/2014 16:00	328.19	324.28
1/8/2014 16:00	322.88	318.26
1/9/2014 16:00	317.56	312.29
1/10/2014 16:00	312.26	306.25
1/11/2014 16:00	306.98	300.27

The differential regression between the eccentric and circular orbits is 0.670° per day which requires 60.9 m/s ΔV to compensate. These values are only about 1% higher than the differential regression and associated ΔV found for the orbit inclined to 50.57°. Next, Table 23 shows the perigee rotation for the orbit inclined to 43.61°.

Table 23: Perigee Rotation with HPOP and Inclination 43.61°

<u>Time (UTCG)</u>	<u>Arg of Perigee (deg)</u> <u>[HPOP]</u>
1/1/2014 16:00	359.89
1/2/2014 16:00	5.82
1/3/2014 16:00	13.33
1/4/2014 16:00	18.83
1/5/2014 16:00	25.97
1/6/2014 16:00	34.11
1/7/2014 16:00	39.89
1/8/2014 16:00	46.60
1/9/2014 16:00	53.89
1/10/2014 16:00	59.43
1/11/2014 16:00	65.18

The perigee rotation averages 6.53° per day over the ten day simulation and requires 27.4 m/s of ΔV per day to compensate. Again, these values for perigee rotation and ΔV are higher than those observed for the orbit inclined to 50.57° with over a 60% gain in ΔV required.

If perigee is left uncontrolled, the maneuvering satellite's altitude over the target will increase over time. Table 24 shows this altitude increase over a ten day period as perigee rotates at 6.53° per day away from the target latitude.

Table 24: Altitude Over Target Latitude as a Function of True Anomaly (ν) at Inclination 43.61°

	ν (degrees)	r (km)	alt (km)
	0.0	6553	175
After 1 Day	6.5	6554	176
After 2 Days	13.1	6558	180
After 3 Days	19.6	6565	187
After 4 Days	26.1	6574	196
After 5 Days	32.6	6585	207
After 6 Days	39.2	6598	220
After 7 Days	45.7	6614	236
After 8 Days	52.2	6631	253
After 9 Days	58.8	6651	273
After 10 Days	65.3	6671	293

Increased altitude over the target and is even more pronounced in the lower inclination (compared to Table 14) due to the higher rate of perigee rotation. By the tenth day, altitude over the target increases by 20 km/day.

Simulating the atmospheric losses at 43.61° will complete the analysis necessary to build special stationkeeping budgets for the maneuvering satellite. The same method was used to determine the final apogee altitudes for the four time periods with varying coefficients of drag as in Table 15. The results are shown in Table 25 for final apogee altitude of orbits inclined to 43.61° .

Table 25: Apogee Altitude for Inclination 43.61°

Start	Stop	Minimum Apogee Altitude (km)		
(mm/dd/yy hh:mm)	(mm/dd/yy hh:mm)	$c_d = 1.8$	$c_d = 2.0$	$c_d = 2.2$
3/30/2001 16:00	4/9/2001 16:00	481.7	468.0	453.7
10/25/2003 16:00	11/4/2003 16:00	490.4	478.0	465.1
11/1/2003 16:00	11/11/2003 16:00	509.8	500.1	489.7
3/30/2009 16:00	4/9/2009 16:00	534.2	528.2	522.1

The atmospheric losses in the orbit inclined to 43.61° are less than the orbit inclined to 50.57° . The ΔV associated with boosting apogee after ten days of operations for the March 2009 (solar minimum) and March 2001 (solar maximum) time periods are 18.3 m/s and 40.7 m/s, respectively.

The new daily ΔV budget for the special stationkeeping during solar minimum conditions is captured in the table below.

Table 26: Daily ΔV Budget for Inclination 43.61°

	Solar Min	Solar Max
	(m/s)	(m/s)
RAAN Regression	60.9	60.9
Perigee Rotation	27.4	27.4
Atm Losses	1.8	4.1
<u>Daily Total</u>	<u>90.2</u>	<u>92.4</u>

Over the period of one orbit, the required special stationkeeping is 25.8 m/s. When the RAAN is allowed to drift, the daily total decreases to 29.3 m/s and the orbit total is 21.9 m/s. The coverage analysis for a ten day scenario with RAAN drift is shown below.

Table 27: Coverage for Eccentric Orbits at Inclination 43.61° (RAAN Drift, Symmetric)

# Planes	# Satellites	% Time Covered	# of Accesses	Time Avg Gap (sec)	Max Response Time (sec)
Constellation with RAAN Drift (one satellite per plane; drift of 6.70 degrees)					
3	6	3.15%	227	5118	13051
Reference Constellation					
3	6	3.14%	226	5001	10122

Table 28: Coverage for Circular Orbits at Inclination 43.61° (RAAN Drift, Symmetric)

# Planes	# Satellites	% Time Covered	# of Accesses	Time Avg Gap (sec)	Max Response Time (sec)
Constellation with RAAN Drift (one satellite per plane; drift of 6.70 degrees)					
3	6	10.55%	281	2584	7401
Reference Constellation					
3	6	10.49%	279	2561	4376

Similarly, if we choose to control RAAN but allow perigee to drift, the ΔV required per orbit is 24.0 m/s. A complete table for all ΔV budgets is included in Appendix B.

4.9. Example Scenario

Imagine a natural disaster occurring in Dayton, Ohio, such as wildfires with conditions changing so quickly that those leading evacuation and recovery efforts need surveillance updates every 2-3 hours. Let us assume that six NanoEye satellites are ready for launch and are stacked in pairs atop three launch vehicles. The rockets are launched and successfully deliver the NanoEye pairs to three planes equally spaced in RAAN and in circular orbits (600 km) inclined to 43.61° . After a brief on-orbit checkout, one satellite in each plane is commanded to perform a phasing maneuver to assume a position in the orbit 180° from the other satellite in the plane. The satellites are each given a two-

digit name; the first digit refers to the plane of the orbit (1, 2, or 3) and the second digit distinguishes between the two satellites in the plane (a or b). The satellites completing the phasing maneuvers are 1b, 2b, and 3b. As each satellite reaches its assigned orbital position, collection of imagery begins at approximately 1.5 meter resolution.

As the first images are received by the users it is realized that recovery efforts will require imagery with sub-meter resolution. Satellites 1a, 2a, and 3a are commanded to maneuver into eccentric orbits to collect high resolution images (up to NIIRS 6). These satellites correct perigee rotation each day to maintain perigee over the target latitude. Also, the maneuvering satellites perform a correction for RAAN and boost apogee altitude once per day. The (a) satellites remain in eccentric orbits until the operation is complete.

Day two of the operation requires extensive coordination and satellites 1b, 2b, and 3b maneuver to eccentric orbits for 24 hours. While all satellites are in eccentric orbits, there is no differential regression of the RAAN so no correction is needed. Altitude corrections must be made for all six satellites, but perigee correction is only required for satellites 1a, 2a, and 3a.

During the third day of surveillance satellites 1b and 3b are commanded to perform a maneuver to eccentric orbits coordinated with the first daylight pass of each satellite. Each satellite will remain in the eccentric orbit for three orbits and then return to the circular orbit. Perigee rotation will not be corrected, but RAAN and altitude will be corrected after apogee is raised to 600 km.

During the sixth and ninth days 1b and 3b are again commanded to maneuver to complete three eccentric orbits coinciding with the first daylight pass over the target.

Operations subside during the tenth day and the (a) satellites are commanded to return to circular orbits. Table 29 shows the ΔV budget for each (a) satellite over the period of operations assuming solar minimum conditions throughout the scenario.

Table 29: Example Scenario: ΔV Budgets for Satellites 1a, 2a, and 3a

	Satellite					
	1a		2a		3a	
	ΔV (m/s)	<i>running total</i>	ΔV (m/s)	<i>running total</i>	ΔV (m/s)	<i>running total</i>
Day 1	120+90	210	120+90	210	120+90	210
Day 2	29	239	29	239	29	239
Day 3	90	329	90	329	90	329
Day 4	90	419	90	419	90	419
Day 5	90	509	90	509	90	509
Day 6	90	599	90	599	90	599
Day 7	90	689	90	689	90	689
Day 8	90	779	90	779	90	779
Day 9	90	869	90	869	90	869
Day 10	120+90+103	1216	120+90+103	1216	120+90+103	1216

The ΔV budget for satellites 1a, 2a, and 3a are identical and each total 1216 m/s for the ten day scenario. The daily ΔV budget for day one includes the initial maneuver to drop perigee to 175 km (120 m/s ΔV), and the stationkeeping requirements for the day (90 m/s). Day 2 requires less ΔV (29 m/s, see Appendix B for Table) because all of the satellites in the constellation are in eccentric orbits and therefore no differential RAAN regression occurs. 90 m/s is added each day after day two to compensate for differential regression of the RAAN, perigee rotation, and atmospheric losses (from Table 26).

Similarly, the final day adds another 120 m/s to circularize the orbit; the phasing maneuver (103 m/s ΔV) is also added to the last day (from Table 16).

Next, the Δv budgets are shown for satellites 1b, 2b, and 3b.

Table 30: Example Scenario: ΔV Budgets for Satellites 1b, 2b, and 3b

	Satellite					
	1b		2b		3b	
	ΔV (m/s)	<i>running total</i>	ΔV (m/s)	<i>running total</i>	ΔV (m/s)	<i>running total</i>
Day 1	202	202	202	202	202	202
Day 2	239+1.8+103	546	239+1.8+103	546	239+1.8+103	546
Day 3	239+3*24	857	0	546	239+3*24	857
Day 4	0	857	0	546	0	857
Day 5	0	857	0	546	0	857
Day 6	239+3*24	1168	0	546	239+3*24	1168
Day 7	0	1168	0	546	0	1168
Day 8	0	1168	0	546	0	1168
Day 9	239+3*24	1479	0	546	239+3*24	1479
Day 10	0	1479	0	546	0	1479

Satellites 1b and 3b have identical ΔV budgets and satellite 2b only maneuvered on days one and two. During day one, each (b) satellite performed a phasing maneuver to take its place in the constellation. The ΔV to perform this phasing maneuver is 202 m/s from Table 16. The 239 m/s ΔV accounts for the maneuver from a circular to eccentric orbit and back to circular. The daily ΔV to compensate for atmospheric losses is 1.8 m/s. Finally, the 24 m/s is the required ΔV to compensate for RAAN, atmospheric losses, and phasing, per orbit. There was no need to correct perigee location for the (b) satellites

during this scenario because the longest dipping maneuver was one day and Table 24 shows that only a one kilometer difference in altitude is realized.

Table 31 shows the coverage metrics for the constellation during each day of the scenario. The coverage changes with the state of the constellation. Day one is the same as days four, five, seven, eight and ten. Day two is the only day that all satellites operate in eccentric orbits. Finally, days three six, and nine are identical in coverage metrics, each having five satellites in eccentric orbits.

Table 31: Coverage Metrics for Example Scenario

# Planes	# Satellites	% Time Covered	Average # of Accesses per Day	Time Avg Gap (sec)	Max Response Time (sec)
Day 1					
3	6	6.88%	25.4	4122	10339
Day 2					
3	6	3.14%	22.6	5001	10122
Day 3					
3	6	4.38%	23.5	4655	12549
Day 4					
3	6	6.88%	25.4	4122	10339
Day 5					
3	6	6.88%	25.4	4122	10339
Day 6					
3	6	4.38%	23.5	4655	12549
Day 7					
3	6	6.88%	25.4	4122	10339
Day 8					
3	6	6.88%	25.4	4122	10339
Day 9					
3	6	4.38%	23.5	4655	12549
Day 10					
3	6	6.88%	25.4	4122	10339

Coverage time decreases as more satellites operate in eccentric orbits. The decreased altitude while over the target decreases the duration of the access. However, Figure 13 shows that slant range to the target is less for satellites operating in eccentric orbits. This results in higher resolution images. The maximum response time of over 12,500 seconds on day three is a result of the satellite pairs converging on in the orbital planes. This clustering cannot be avoided when one satellite in the plane is in an eccentric orbit and one satellite is in a circular orbit. Eventually, the satellite with the shorter period will overtake the other satellite. The Time Average Gap between accesses is not drastically affected by the dynamic configuration of the constellation.

Table 29 and Table 30 show the ΔV used during the scenario, subtracting the scenario total from the total ΔV available on the satellites leaves the remaining ΔV . The (a) satellites expended nearly half of their propellant and have approximately 1.3 km/s ΔV available for future operations. Satellites 1b and 3b retain approximately 1.0 km/s ΔV and satellite 2b has almost 2.0 km/s ΔV after the scenario ends. The most surprising result is that satellites 1b and 3b expended more propellant than the (a) satellites. This indicates that during periods of prolonged operations, satellites should remain in eccentric orbits to avoid the cost of maneuvering between the orbits.

At the conclusion of the scenario all six satellites have enough ΔV to support future operations. The New SMAD estimates ΔV requirements between 15 m/s and 75 m/s per year for general stationkeeping and between 120 m/s and 150 m/s for controlled re-entry. After satellites 1a, 1b, 2a, 3a, and 3b reach their end of life, satellite 2b could be used to augment future constellations or act as an on-orbit spare.

V. Conclusions and Recommendations

5.1. Introduction

The objective of this thesis is to determine if a responsive constellation of Earth imaging satellites is feasible for surveillance of natural disasters and combat operations in areas of denied access. The Army's Space and Missile Defense Command (SMDC) has proposed a system called NanoEye to provide National Imagery Interpretability Rating Scale (NIIRS) 6 images directly to tactical ground forces in near real-time. Similarly, Hong, et al, have proposed that the Disaster Monitoring Constellation (DMC) be extended to operate in a disaster mode where satellites currently in orbit would maneuver to lower orbits and provide higher resolution images than those currently available. The Defense Advance Research Projects Agency (DARPA) is pursuing a concept called SeeMe that would provide similar results from small satellites in very low circular orbits.

The low cost of building and deploying small satellites makes it tempting to abandon the paradigm of 'big space,' or at least augment it during times of crisis. Future leaders may launch a constellation of small satellites tailored for a specific operation, that is, if economic and technical feasibility can be demonstrated. These constellations would measure reliability at the system level and accept failure of individual satellites without compromising the end product.

The unique quality of NanoEye is the use of elliptical orbits and low altitude passes to collect high resolution images. Operating satellites in eccentric low Earth orbits (LEO) and especially at altitudes below 200 km introduces perturbations that must be considered in order to predict the ΔV required for constellation management.

5.2. Inclination

The objective of NanoEye is to offer frequent and regular coverage of a target. The inclination into which the satellites are launched will substantially affect the coverage provided by the constellation (see Table 21). Some important metrics of coverage are: number of satellite passes; time average gap; and maximum revisit time. When a satellite's orbit is inclined to the sum of the target latitude and the Earth central angle, these metrics are optimized. However, the Earth central angle is a function of altitude, and NanoEye is not planned to operate at a constant altitude. For this reason, the user must decide into which orbital inclination the satellites will be launched. If a satellite operates in an eccentric orbit (perigee over the target latitude) for the majority of its life, then the inclination should be optimized for an orbit altitude of 175 km. If a satellite is anticipated to operate for extended periods of time in the circular (600 km) orbit, the user may choose to optimize coverage for this higher altitude. It is possible to use propellant to change the inclination of the orbit but the maneuver would use almost 1 km/s of the 2.5 km/s of available ΔV .

Choosing the wrong inclination can significantly impact the coverage metrics of the constellation. However, Table 21 shows that impact of choosing the wrong inclination is less damaging if the user launches into 43.61° inclination. This makes the lower inclination the better choice unless unforeseen events place targets outside the satellite's field of view.

5.3. Coverage

Maneuvering from 600 km circular orbits to eccentric orbits with apogee at 600 km and perigee at 175 km drastically increases the image resolution by decreasing the slant range to the target. As the satellite passes the target at a lower altitude, the satellite footprint becomes smaller and the duration of access decreases. These factors contribute to a decrease in coverage time for satellites in eccentric orbits compared to those in circular orbits, but the images collected at lower altitude produce images at higher NIIRS levels (see Figure 13).

Satellites in the eccentric orbits also provide fewer accesses to the target and consequently show an increase in time average gap and maximum response time (Table 21). However, coverage metrics degrade to a higher degree at an inclination of 50.57° compared to an inclination of 43.61° . The lower inclination is optimized to the low altitude pass and allows for an 85% increase in accesses over the ten day sample scenario. Maneuvering satellites to a lower orbit must be done only when increased image resolution is required. Degraded coverage metrics are an unavoidable consequence of operating in the eccentric orbits. When satellites are maneuvered from circular to eccentric, and then back to circular orbits, coverage may continue to be degraded compared to the original (symmetric) constellation if perturbations are not counteracted.

When individual planes within a constellation drift away from their symmetric positions, the first coverage metric to degrade is maximum response time. Table 11 shows a 50% increase in maximum response time for a constellation of circular orbits at 50.57° with one satellite in each of the three planes having 5.91° RAAN drift from symmetry.

Stationkeeping should be accomplished to maintain the symmetry of the constellation and preserve the coverage metrics it provides.

5.4. Constellation

The NanoEye system seeks to provide non-continuous regional coverage. A symmetric Walker Delta constellation provides the best coverage metrics for this case. Though the size of the constellation is not precisely known, it is assumed that six satellites will launch initially and may be augmented by additional satellites as necessary to reach desired coverage metrics. Examining only the first six satellites, constellation design reduces to determining the number of planes. The constellation must have one, two, three, or six planes to remain symmetric (each plane having an equal, integer number of satellites). These four configurations were examined using Turner's equation to determine the optimal phasing parameter of each. By far, the worst coverage was provided by placing all six satellites in a single plane. A two plane configuration, each containing three satellites, had excessive maximum response time compared to three and six plane configurations (see Table 7). Three and six plane constellations had similar coverage characteristics with the three plane configuration gaining preference due to a time average gap approximately 20% less than the six plane configuration.

Launching into multiple planes requires either expensive plane change maneuvers or multiple launch vehicles. Many options are available for launch; four possible launch vehicles will be introduced but many more exist. The Army began development on a launch vehicle called the Multipurpose NanoMissile System capable of delivering 10 kg to LEO for approximately \$1M per launch. Similarly, DARPA has awarded contracts to

develop a launch vehicle capable of delivering 100 pounds to LEO for \$1M (see Figure 14).



Figure 14: DARPA ALASA (Artist's Concept)

Sandia National Labs is developing a launch vehicle called the Super Strypi that seeks to provide low cost access to LEO and satisfy requirements for short-notice launches.

Commercial platforms are also available such as Orbital Science's Pegasus which can easily deliver a pair of small satellites to LEO. To meet budgetary goals and operational timelines, though, the government intends to develop these systems organically.

Assuming that light-lift space launch platforms will be available at a reasonable cost, constellations with one or two satellites per plane provide more robust coverage for contingency operations.

5.5. Eccentric Orbits

Maneuvering from a circular orbit to an eccentric orbit has implications on propellant use far greater than the ΔV necessary to lower perigee. The orbit of the maneuvering satellite will have a differential regression of the RAAN (Table 8) compared to satellites in circular orbits. Also, the argument of perigee will rotate in the plane of the orbit (with the exception of orbits inclined to 63.4° , see Figure 8). Lastly, apogee altitude will be degraded due to atmospheric drag experienced at perigee. The first two perturbations are most significantly affected by J_2 , but also show noticeable differences caused by higher order perturbations.

The maneuvering satellite must either return to the circular orbit (600 km) or drag will force the satellite to re-enter the atmosphere in a matter of weeks. In the more desirable scenario in which the satellite returns to the circular orbit, the coverage metrics will be degraded if the plane of the orbit is offset compared to the symmetric constellation. For example, in a three plane constellation with each plane containing two satellites, if one satellite from each plane maneuvers and does not compensate for differential RAAN regression, the maximum response time will increase by 50% (see Table 11). However, if every satellite in the constellation were maneuvered together, there would be no differential regression. The entire constellation would rotate as a system and the relative spacing of the satellites would go unchanged even after returning to circular orbits. If the majority of the satellites in a constellation maneuver to the eccentric orbit, it would be more economical to adjust the RAAN of the remaining satellites to match that of the majority after the dipping maneuver was complete. RAAN

differences and atmospheric losses should be counteracted to maintain symmetry of the constellation and preserve the coverage metrics.

In contrast, perigee rotation does not permanently affect the coverage of the constellation. After satellites maneuver back to the circular orbit, perigee is not defined and can be forgotten. Perigee location is only a concern while in the eccentric orbit, affecting image resolution more than coverage. Perigee rotation increases the altitude at which the satellite overflies the target, thereby reducing the image resolution obtainable. The range between the target and the satellite as a function of perigee rotation is calculated using Equation 21 and can be seen in Table 14 and Table 24. Perigee rotation should not be corrected if the satellite maneuvers to an eccentric orbit for two days or less. After two days, the difference in range may significantly impact the image resolution. A methodology is described in section 5.9 to determine when a maneuver is required based on range thresholds set by the user. Without any further analysis though, it can be concluded that the average slant range would be minimized if the satellite were commanded to dip perigee in advance of the target and allow the perturbations to rotate perigee over the target during the following orbits. For example, if a three day maneuver was conducted at 43.61° , the perigee would drift approximately 19.6° . If the initial location of perigee was placed 9.8° in advance of the target then the final position of perigee would be 9.8° past the target, thereby reducing the maximum angular error by 50%.

5.6. Atmospheric Drag

Apogee altitude decreases as satellites maneuver within the atmosphere. The drag imparted on the satellite will depend on atmospheric conditions. During solar maximum and solar storming the atmosphere expands and exerts a drag force at altitudes not typically affected. Estimating atmospheric drag must be done broadly to account for varying atmospheric and solar conditions. Over a ten day period, a satellite with an apogee altitude of 600 km and a perigee altitude of 175 km will likely decay to an apogee altitude between 446 km and 534 km. As the altitude of apogee decreases the orbital period also decreases. The most efficient method to return the maneuvering satellite to a circular orbit is to perform a ΔV maneuver first at apogee to boost perigee to 600 km and then perform another maneuver 180 degrees later in Mean Anomaly (at the new apogee) to circularize the orbit at 600 km. The first recovery maneuver will be roughly equivalent to the ΔV that maneuvered the satellite from the circular to the eccentric orbit in the first place; the second maneuver will vary depending on the decay of apogee.

5.7. ΔV Budgets

Appendix B summarizes the ΔV requirements per day and per orbit under specific assumptions, as noted, for the two orbital inclinations discussed. The only clear conclusion from the ΔV analysis is that energy must be added to the orbit to compensate for atmospheric losses, otherwise the satellite will be destroyed. The decision to compensate for regression of the RAAN depends on the users' desire to preserve coverage metrics of the symmetric constellation. Finally, the rotation of perigee primarily affects image resolution and must be corrected based on thresholds set by the user.

Additionally, if a particular satellite was nearing its end of life, it should be permitted to drift rather than deplete its final propellant. A final consideration for propellant management may reside in the number of replacements ready for launch. The operators may be more willing to expend propellant for a slightly better image if another satellite is ready to replenish the constellation, or if an on-orbit spare was already in place.

As the constellation grows, the need for strict constellation management diminishes. The size of the constellation will drive down the average and maximum response times and allowing RAAN to drift will not impact the coverage metrics as drastically as was noticed in the six satellite system (see Appendix D). Understanding this trade-space is essential to the successful management of the system.

5.8. Significance of Research

Constellations of maneuvering satellites have been the focus of research and development in recent years but specific ΔV requirements for such systems have not yet been published. This research has quantified the ΔV budget for multiple concepts of operation. The example scenario in section 4.9 quantifies the ΔV required for a specific operation that may be a typical use of the NanoEye system.

STK was used to model the orbits and an analytical solution for the J_2 perturbations validated the results. Coverage metrics in STK were also validated against a MATLAB program written by Kimberly Sugrue as part of her 2007 AFIT thesis on a similar topic.

The specifications proposed by SMDC for NanoEye performed well in the example scenario and provide a feasible solution for contingency operations.

5.9. Recommendations for Future Work

The modelling of atmospheric forces in STK was not validated in this research. A PhD candidate at AFIT is modelling the atmosphere in MATLAB, using the NRLMSISE-00 model directly, and has validated STK results for scenarios relative to his research. The title of the student's prospectus is *The Prospect of Operationally Responsive Space Using Atmospheric Skip Entry Maneuvers*.

In order to model atmospheric forces in STK, the coefficient of drag of NanoEye was estimated based on historical data. The actual coefficient of drag is proprietary and was not released by the designers of the satellite. A sensitivity analysis was completed to quantify the range of possible solutions due to the uncertainty in c_d (Table 15 and Table 25). As more information is publicly released and as relationships mature between SMDC and AFIT, this information may become available for more detailed modelling.

This thesis describes a six satellite constellation but the operational system is expected to have as many as 12 satellites, or perhaps more. Coverage metrics for a 12 satellite constellation should be studied to determine if ΔV requirements for maneuvering can be decreased (this analysis has been started, see Appendix D). The majority of the daily ΔV budget was expended to offset the differential regression of the RAAN. If a sufficient number of satellites was fielded in the constellation so that RAAN could be allowed to drift, the life of each satellite could be significantly extended. Additionally,

coverage gap analysis could be performed to fill gaps in coverage and drive down the maximum revisit time in these constellations.

Further research may also examine perigee rotation more closely. Vallado outlines “Minimum Altitude Variation Orbits” where thresholds are defined for variations in apogee altitude over a target. A maximum change in altitude is determined and then related to perigee rotation. Using the perigee rotation rate, it is possible to determine the frequency of corrections necessary to stay within a tolerance band of altitudes over the target. The goal of NanoEye is to place perigee over the target at an altitude of 175 km, but the range of acceptable values is not known at this time.

Thomas Co’s dissertation presents a method for adjusting the ground track and time of arrival of maneuvering spacecraft to intersect pre-planned targets. Co’s method may be used to intersect the ground track with the target for an otherwise near-miss. Direct over flight of the target allows for the shortest possible slant range and therefore the best resolution achievable.

Another area of research is the distribution of information within the constellation. It should be clear how a tactical user will task the constellation for imagery of a particular target. Presumably, the request will be received by the closest satellite in the constellation and then passed through cross-links to another satellite that will soon overfly the target. The user will want confirmation that the request has been received and may need to know when the image will be delivered. The challenge with maneuvering satellites is maintaining situational awareness within the constellation so that the satellite receiving the request knows how to hand off the request. *Mesh Networking of Small Low Earth Orbit Satellites* by Siraj and Yahiro suggests a method for routing information

within a LEO constellation of communications satellites. The authors describe the system as a “deterministic configuration,” which differs from the NanoEye concept when maneuvering is introduced. Knowledge of maneuvers must be shared within the constellation and the new orbits must be propagated in near real-time in order to manage user requests.

Appendix A

Accounting for Atmospheric Effects (drag) in LEO

HPOP:

In Properties/Basic/Orbit, click Force Model under the heading Prop Specific and choose the appropriate Atm. Density Model in the Drag section (recommend MSIS 2000). Under SolarFlux/GeoMag choose Use File as opposed to the default Enter Manually and then browse the files under Flux/Ap File. Choose SpaceWeather-All-v1.2.txt then choose the appropriate Geomag Update Rate (3 hours) and Flux Source (Kp from file)

In the main STK window click Utilities at the top of the screen and select Data Update from the dropdown menu. Select the check box for SpaceWeather-All-v1.2.txt and choose update now (this may require downloading the file on a non-DoD networked computer and copying the file onto the desired workstation, the filename will be the same but data is updated to the current date)

Also, under Utilities click Data Update and update data set SpaceWeather-All-v-1.2.txt (will give data up to the current date instead of the projections/estimates provided for late 2010-present).

Astrogator:

Under Utilities choose Component Browser on the dropdown menu and then select Atmospheric Models under the Propagation Functions expansion (+) button.

Duplicate the NRLMSISE 2000 and give it an appropriate name (NRLMSISE 2000 with Atmosphere). Double click the component just created and change the source

under SolarFlux/GeoMag to Data File and choose the File: SpaceWeather-All-v1.2.txt (update every 3 hours, read Kp from file).

Then duplicate the actual propagator 'Earth HPOP Default v8-1-1' (now Earth HPOP Default v8-1-1 with Atmosphere) and edit to include the newly created NRLMSISE 2000 with values from file instead of the default Jacchia-Roberts model (this must be removed before the new atmospheric model can be added).

Also, under Utilities click Data Update and update data set SpaceWeather-All-v-1.2.txt (will give data up to the current date instead of the projections/estimates provided for late 2010-present).

Modeling Specific to NanoEye

The frontal area of the NanoEye satellite was calculated using values from Wertz's paper "NanoEye -- Military Relevant Surveillance." The values are L=1.8 m, W=0.7 m, and D=0.3 m. This gave an area of 0.21 m². The dry mass of the satellite is 20 kg and the wet mass is 80 kg. A mass of 50 kg was used in the model to simulate a half-full propellant tank. Therefore, the value used for Area/Mass Ratio was 0.0042 m²/kg.

The NanoEye satellite was modelled as a solid cylinder for purposes of modelling the moments of inertia (MOI). The equations used are listed:

$$I_x = I_y = \frac{1}{12} m (3 r^2 + h^2) \quad (23)$$

$$I_z = \frac{1}{2} m r^2 \quad (24)$$

where m is mass, h is the height of the cylinder (length of the satellite measured in the direction of the velocity vector), and r is the radius of the unibody tank structure. The radius was assumed to be 0.5 m. Then the values for MOI are as follows:

$$I_x = I_y = 14.281$$

$$I_z = 1.563$$

Lastly, a coefficient of drag (c_d) of 2.0 was assigned to NanoEye, even though the exact value is unpublished.

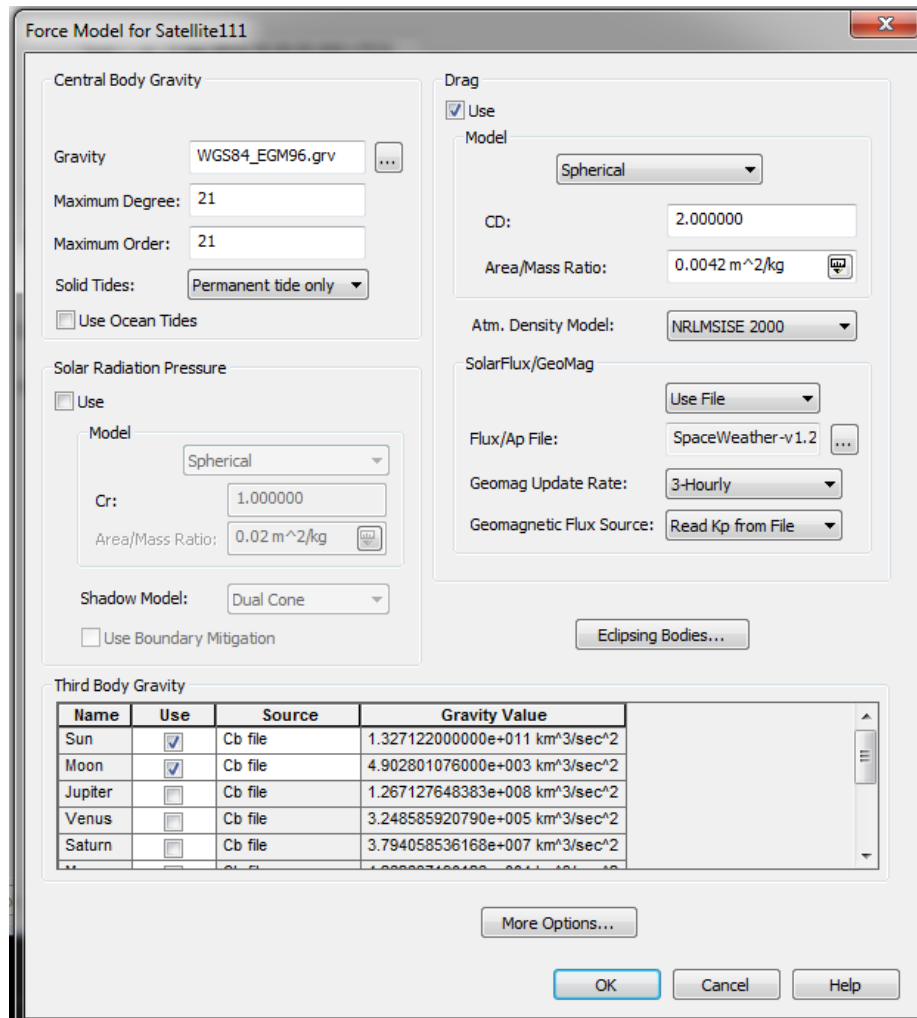


Figure 15: STK Force Model (Atmosphere)

Appendix B

ΔV budgets for 50.57° and 43.61° symmetric Walker constellations (ΔV budget is per satellite).

See tables on the pages that follow.

Table 32: ΔV Budget for $i = 50.57^\circ$ (RAAN, Perigee, Atm)

<u>Correcting for RAAN, Perigee and Atm</u>		
Inclination	50.57	degrees
Orbital Period	0.0641	days
	(m/s)	(m/s)
Dip and Recover	239	239
Average Phasing	103	103
<u>ΔV budget per day</u>		
	Solar Min	Solar Max
	(m/s)	(m/s)
RAAN Regression	60.2	60.2
Perigee Rotation	17.1	17.1
Atm Losses	2.0	4.3
<u>Daily Total</u>	<u>79.3</u>	<u>81.6</u>
<u>ΔV budget per orbit</u>		
	Solar Min	Solar Max
	(m/s)	(m/s)
RAAN Regression	3.9	3.9
Perigee Rotation	1.1	1.1
Atm Losses	0.1	0.3
Phasing Maneuver	20.0	20.0
<u>Orbit Total</u>	<u>25.1</u>	<u>25.2</u>
<u>Running Daily Total</u>		
	Solar Min	Solar Max
	(m/s)	(m/s)
After 1 Day	421	424
After 2 Days	501	505
After 3 Days	580	587
After 4 Days	659	668
After 5 Days	738	750
After 6 Days	818	832
After 7 Days	897	913
After 8 Days	976	995
After 9 Days	1055	1076
After 10 Days	1135	1158

Table 33: ΔV Budget for $i = 50.57^\circ$ (Perigee, Atm)

Correcting for Perigee and Atm		
Inclination	50.57	degrees
Orbital Period	0.0641	days
	(m/s)	(m/s)
Dip and Recover	239	239
Average Phasing	103	103
<u>ΔV budget per day</u>		
	Solar Min	Solar Max
	(m/s)	(m/s)
RAAN Regression	--	--
Perigee Rotation	17.1	17.1
Atm Losses	2.0	4.3
<u>Daily Total</u>	<u>19.1</u>	<u>21.4</u>
<u>ΔV budget per orbit</u>		
	Solar Min	Solar Max
	(m/s)	(m/s)
RAAN Regression	--	--
Perigee Rotation	1.1	1.1
Atm Losses	0.1	0.3
Phasing Maneuver	20.0	20.0
<u>Orbit Total</u>	<u>21.2</u>	<u>21.4</u>
<u>Running Daily Total</u>		
	Solar Min	Solar Max
	(m/s)	(m/s)
After 1 Day	361	363
After 2 Days	380	385
After 3 Days	399	406
After 4 Days	418	428
After 5 Days	437	449
After 6 Days	456	470
After 7 Days	475	492
After 8 Days	494	513
After 9 Days	514	535
After 10 Days	533	556

Table 34: ΔV Budget for $i = 50.57^\circ$ (RAAN, Atm)

<u>Correcting for RAAN and Atm</u>		
Inclination	50.57	degrees
Orbital Period	0.0641	days
	(m/s)	(m/s)
Dip and Recover	239	239
Average Phasing	103	103
<u>ΔV budget per day</u>		
	Solar Min	Solar Max
	(m/s)	(m/s)
RAAN Regression	60.2	60.2
Perigee Rotation	--	--
Atm Losses	2.0	4.3
<u>Daily Total</u>	<u>62.2</u>	<u>64.5</u>
<u>ΔV budget per orbit</u>		
	Solar Min	Solar Max
	(m/s)	(m/s)
RAAN Regression	3.9	3.9
Perigee Rotation	--	--
Atm Losses	0.1	0.3
Phasing Maneuver	20.0	20.0
<u>Orbit Total</u>	<u>24.0</u>	<u>24.1</u>
<u>Running Daily Total</u>		
	Solar Min	Solar Max
	(m/s)	(m/s)
After 1 Day	404	406
After 2 Days	466	471
After 3 Days	528	535
After 4 Days	591	600
After 5 Days	653	664
After 6 Days	715	729
After 7 Days	777	793
After 8 Days	839	858
After 9 Days	901	922
After 10 Days	964	987

Table 35: ΔV Budget for $i = 43.61^\circ$ (RAAN, Perigee, Atm)

<u>Correcting for RAAN, Perigee and Atm</u>		
Inclination	43.61	degrees
Orbital Period	0.0641	days
	(m/s)	(m/s)
Dip and Recover	239	239
Average Phasing	103	103
<u>ΔV budget per day</u>		
	Solar Min	Solar Max
	(m/s)	(m/s)
RAAN Regression	60.9	60.9
Perigee Rotation	27.4	27.4
Atm Losses	1.8	4.1
<u>Daily Total</u>	<u>90.2</u>	<u>92.4</u>
<u>ΔV budget per orbit</u>		
	Solar Min	Solar Max
	(m/s)	(m/s)
RAAN Regression	3.9	3.9
Perigee Rotation	1.8	1.8
Atm Losses	0.1	0.3
Phasing Maneuver	20.0	20.0
<u>Orbit Total</u>	<u>25.8</u>	<u>25.9</u>
<u>Running Daily Total</u>		
	Solar Min	Solar Max
	(m/s)	(m/s)
After 1 Day	432	434
After 2 Days	522	527
After 3 Days	613	619
After 4 Days	703	712
After 5 Days	793	804
After 6 Days	883	897
After 7 Days	973	989
After 8 Days	1064	1081
After 9 Days	1154	1174
After 10 Days	1244	1266

Table 36: ΔV Budget for $i = 43.61^\circ$ (Perigee, Atm)

Correcting for Perigee and Atm		
Inclination	43.61	degrees
Orbital Period	0.0641	days
	(m/s)	(m/s)
Dip and Recover	239	239
Average Phasing	103	103
<u>ΔV budget per day</u>		
	Solar Min	Solar Max
	(m/s)	(m/s)
RAAN Regression	--	--
Perigee Rotation	27.4	27.4
Atm Losses	1.8	4.1
<u>Daily Total</u>	<u>29.3</u>	<u>31.5</u>
<u>ΔV budget per orbit</u>		
	Solar Min	Solar Max
	(m/s)	(m/s)
RAAN Regression	--	--
Perigee Rotation	1.8	1.8
Atm Losses	0.1	0.3
Phasing Maneuver	20.0	20.0
<u>Orbit Total</u>	<u>21.9</u>	<u>22.0</u>
<u>Running Daily Total</u>		
	Solar Min	Solar Max
	(m/s)	(m/s)
After 1 Day	371	374
After 2 Days	401	405
After 3 Days	430	437
After 4 Days	459	468
After 5 Days	488	500
After 6 Days	518	531
After 7 Days	547	563
After 8 Days	576	594
After 9 Days	605	626
After 10 Days	635	657

Table 37: ΔV Budget for $i = 43.61^\circ$ (RAAN, Atm)

<u>Correcting for RAAN and Atm</u>		
Inclination	43.61	degrees
Orbital Period	0.0641	days
	(m/s)	(m/s)
Dip and Recover	239	239
Average Phasing	103	103
<u>ΔV budget per day</u>		
	Solar Min	Solar Max
	(m/s)	(m/s)
RAAN Regression	60.9	60.9
Perigee Rotation	--	--
Atm Losses	1.8	4.1
<u>Daily Total</u>	<u>62.8</u>	<u>65.0</u>
<u>ΔV budget per orbit</u>		
	Solar Min	Solar Max
	(m/s)	(m/s)
RAAN Regression	3.9	3.9
Perigee Rotation	--	--
Atm Losses	0.1	0.3
Phasing Maneuver	20.0	20.0
<u>Orbit Total</u>	<u>24.0</u>	<u>24.2</u>
<u>Running Daily Total</u>		
	Solar Min	Solar Max
	(m/s)	(m/s)
After 1 Day	405	407
After 2 Days	468	472
After 3 Days	530	537
After 4 Days	593	602
After 5 Days	656	667
After 6 Days	719	732
After 7 Days	781	797
After 8 Days	844	862
After 9 Days	907	927
After 10 Days	970	992

Appendix C

Minimum Slant Range to Target observed during a ten day scenario with six satellites orbiting in eccentric orbits (175 km by 600 km), at 50.57° and 43.61°:

Table 38: Minimum Slant Range to Target at Inclination 50.57°

$i=50.57^\circ$	Minimum Slant Range to Target (km)					
Access #	Satellite1	Satellite2	Satellite3	Satellite4	Satellite5	Satellite6
1	189	185	186	184	184	192
2	207	214	201	188	221	201
3	254	248	251	209	223	262
4	302	284	281	236	239	270
5	317	302	317	306	310	317
6	328	315	329	315	313	321
7	334	333	360	331	314	360
8	364	352	368	333	328	362
9	373	363	380	345	333	378
10	386	387	384	356	343	392
11	405	407	397	395	395	436
12	430	410	436	427	415	448
13	440	474	482	436	424	468
14	452	493	491	437	461	478
15	458	494	509	480	479	525
16	543	497	526	543	538	601
17	556	517	602	555	571	604
18	636	590	609	649	647	618
19	694	623	695	678	673	693
20	843	683	751	827	792	718
21		767				745

Table 39: Minimum Slant Range to Target at Inclination 43.61°

$i=43.61^\circ$	Minimum Slant Range to Target					
Access #	Satellite1	Satellite2	Satellite3	Satellite4	Satellite5	Satellite6
1	188	189	189	190	191	188
2	189	194	200	197	194	204
3	198	214	211	220	219	208
4	209	233	237	231	226	240
5	234	256	248	267	226	255
6	264	277	253	270	262	275
7	275	278	276	276	277	283
8	279	279	281	276	281	286
9	284	298	291	283	291	293
10	286	299	296	287	294	308
11	312	302	300	291	310	316
12	320	303	307	315	311	326
13	327	329	332	315	318	332
14	343	341	338	316	324	333
15	347	347	342	349	353	335
16	363	349	368	350	355	336
17	376	365	381	360	355	371
18	379	384	396	374	359	377
19	383	389	397	386	389	389
20	404	394	403	401	397	406
21	411	417	411	420	423	407
22	438	422	419	436	426	409
23	438	427	430	436	427	415
24	442	453	435	444	452	438
25	458	456	445	445	456	442
26	466	470	451	459	457	460
27	468	477	458	470	472	465
28	483	479	472	482	480	469
29	487	492	479	489	491	470
30	488	493	480	497	496	482
31	498	495	491	501	502	489
32	499	503	496	505	504	497
33	506	503	502	506	505	501
34	506	503	505	507	507	505
35	533	507	507	526	516	506
36	552	583	576	628	617	565
37	636	692	683	740	707	671
38	749	--	800	--	728	765

Appendix D

Though the focus of this research is on the first six satellites of a dynamic constellation, the end-state of the constellation is unknown. Appendix D explores the coverage metrics for a 12 satellite constellation and specifically examines the degradation of metrics if the RAAN is allowed to drift over a ten day period. Table 40 presents the results of coverage analysis for constellations each containing 12 satellites in circular orbits (600 km altitude) in three, six, and 12 plane configurations, all inclined to 50.57° . These constellations are realistic extensions of the constellations presented in Table 3. One limitation is that the 12 satellite, 12 plane constellation can only be built from the six satellite, six plane constellation without requiring a plane rotation for the satellites already in orbit. As a general rule, the expanded constellation cannot have fewer satellites per plane than the initial constellation without a requiring a plane rotation maneuver. Additionally, the number of planes in the initial constellation must be a factor of the number of planes in the expanded constellation; otherwise a plane rotation maneuver will be required. For example, a two plane constellation cannot be transformed into a three plane constellation without adjusting the RAAN of the satellites in one of the initial planes. The two plane constellation can mature into a four or six plane constellation by adding additional planes with the same number of satellites per plane as in the initial constellation. Lastly, satellites can be added to existing planes, possibly requiring a phasing maneuver of the initial satellites to create uniform spacing within the plane. For example, the six satellite, three plane constellation can expand to a 12

satellite, three plane constellation by adding an additional two satellites per plane and then re-optimizing the inter-plane phasing.

Table 40: Coverage metrics for 12 Satellite Constellations at 50.57° Inclination

Coverage: Symmetric vs. RAAN Shift of 5.91° (6 Satellites Shifted)

# Planes	# Satellites	% Time Covered	# of Accesses	Time Avg Gap (sec)	Max Response Time (sec)	
3	12	19.02%	650	1008	2996	
3	12	19.03%	651	1024	4529	RAAN Shift
6	12	18.86%	646	1200	2018	
6	12	18.84%	649	1199	2066	RAAN Shift
12	12	18.92%	647	2190	3840	
12	12	18.91%	646	2181	3899	RAAN Shift

The coverage metrics for the three plane constellation are very comparable to those shown in Table 11. The maximum response is increased by approximately 50% when RAAN is allowed to drift. The coverage metrics are degraded significantly less for the six and 12 plane constellations compared to the three plane constellation with only a few percent increase in max response time with drifting RAAN.

Table 41 examines the coverage metrics for constellations inclined to 43.61°.

Table 41: Coverage metrics for 12 Satellite Constellations at 43.61° Inclination

Coverage: Symmetric vs. RAAN Shift of 6.70° (6 Satellites Shifted)

# Planes	# Satellites	% Time Covered	# of Accesses	Time Avg Gap (sec)	Max Response Time (sec)	
3	12	21.32%	560	985.5	2395	
3	12	21.28%	557	1038	3887	RAAN Shift
6	12	21.32%	562	1392	2709	
6	12	21.43%	566	1370	2793	RAAN Shift
12*	12	21.34%	559	2759	4482	
12*	12	21.36%	564	2718	4524	RAAN Shift
12**	12	21.31%	558	1712	3122	
12**	12	21.30%	558	1732	3210	RAAN Shift
12***	12	21.36%	561	998	1709	
12***	12	21.35%	565	1001	1792	RAAN Shift

- * phasing parameter 10
- ** phasing parameter of 1
- *** phasing parameter of 2

Additional 12 plane constellations are examined to explore different phasing parameters. Equation 1 calculates an optimal phasing parameter of 10 for the 12 plane constellation. The coverage metrics are worse for a 12/12/10 symmetric constellation compared to both the three and six plane constellations. This result is unexpected but not impossible. The analysis was repeated with phasing parameters of one and two (** and *** in the table). The coverage metrics drastically improved, with the latter easily beating out any other configuration tested. This leads to an additional topic for future research: Does Turner's equation break-down for constellations with more than six planes?

Bibliography

- Adams, W. S., L. Rider. "Circular Polar Constellations Providing Continuous Single or Multiple Coverage Above a Specified Latitude." *Journal of the Astronautical Sciences*, Vol. 35, No. 2. April-June, 1987.
- Campbell, James B., Randolph H. Wynne. *Introduction to Remote Sensing, Fifth Edition*. New York. Guilford Press. 2011.
- Co, Thomas C. *Operationally Responsive Spacecraft Using Electric Propulsion*. Dissertation. AFIT/DS/ENY/12-01. Graduate School of Management and Engineering, Air Force Institute of Technology (AU), Wright-Patterson AFB OH. September 2012.
- Curiel, Alex de Silva, Philip Davies, Stuart Eves, Lee Boland, Martin Sweeting. "Real-Time Mosaic – Rapid Response High-Resolution Imaging from Space." AIAA 2nd Responsive Space Conference, Los Angeles, California. April 2004.
- de Weck, Olivier, Richard de Neufville, Mathieu Chaize. "Staged Deployment of Communications Satellites in Low Earth Orbit." *Journal of Aerospace Computing, Information, and Communication*, Volume 1. March 2004. 119-136.
- Eves, Stuart, Mark Taylor. "Thinking at the Constellation Level." AIAA 8th Responsive Space Conference, Los Angeles, California. March 2010.
- Hanson, John M., Alexander N. Linden. "Improved Low-Altitude Constellation Design Methods." *Journal of Guidance, Control, and Dynamics* (ISSN 0731-5090), vol. 12. Mar-Apr 1989. 228-236.
- Hong, SeungBum, Jaemyung Ahn, Hyungho Na. "Design of the High-Mobility Disaster Monitoring Satellite Constellation Using the Orbiting Depot." AIAA Space Conference, Long Beach, California. September 2011. AIAA Paper 2011-7263.
- Kelley, Clifford, Maged Dessouky. "Minimizing Cost Availability of Coverage from a Constellation of Satellites: Evaluation of Optimization Methods." *Systems Engineering*, Volume 7 Issue 2. June 2004. 113 – 122.
- Kestrel Eye Technology Center. U.S. Army Space & Missile Defense Command / Army Forces Strategic Command. 3 February 2010. www.army.mil/smdc
- Krueger, Jared K., Daniel Selva, Matthew W. Smith, John Keese. "Spacecraft and Constellation Design for a Continuous Responsive Imaging System in Space." AIAA Space Conference, Pasadena, California. September 2009. AIAA Paper 2009-6773.

- Lang, Thomas J. "Low Earth orbit satellite constellations for continuous coverage of the mid-latitudes." AIAA/AAS Astrodynamics Conference, San Diego, CA. July 1996. AIAA Paper 96-3638.
- Lang, Thomas J. "Optimal Low Earth Orbit Constellations for Continuous Global Coverage." Proceedings of the AAS/AIAA Conference, Lake Placid, NY, August 1983. 1071-1086. San Diego: Univelt. 1994.
- Lang, Thomas J. "Symmetric Circular Orbit Satellite Constellations for Continuous Global Coverage." August 1987. AAS Paper 87-499.
- Larrimore, Scott C. "Partially Continuous Earth Coverage from a Responsive Space Constellation." AIAA 5th Responsive Space Conference, Los Angeles, California. April 2007
- Layton, Laura. "Halloween Storms of 2003 Still the Scariest." NASA/News/Solar System. Goddard Space Flight Center. October 2008
http://www.nasa.gov/topics/solarsystem/features/halloween_storms.html
- London, John R., David J. Weeks, Mark E. Ray, A. Brent Marley. "Low Cost Responsive Space for the US Army." Reinventing Space Conference, Los Angeles, California. March 2012.
- London, John R., Richard White, David Weeks, A. Brent Marley. "Army Technical Nanosatellites." Reinventing Space Conference, Los Angeles, California, March 2011.
- Middour, Jay W. "Survey of Orbit Selection for Satellite Earth Surveillance." AIAA Space Technology Conference, Albuquerque, New Mexico. September 1999. AIAA Paper 99-4637.
- NanoEye Technical Center. U.S. Army Space & Missile Defense Command / Army Forces Strategic Command. 28 September 2011. www.army.mil/smdc
- Sauter, Luke M. *Satellite Constellation Design for Mid-Course Ballistic Missile Intercept*. MS thesis. Massachusetts Institute of Technology, Cambridge, MA. June 2004.
- Sellers, Jerry Jon. *Understanding Space*. The McGraw-Hill Companies, Inc. 2007.
- Sidi, Marcel J. *Spacecraft Dynamics and Control: A Practical Engineering Approach*. Cambridge University Press. 2000.
- Siraj, Aimal, Yukie Yashiro. "Mesh Networking of Small Low Earth Orbit Satellites." AIAA 8th Responsive Space Conference, Los Angeles, California. March 2010.

- Sugrue, Kimberly. *Optimal Orbital Coverage of Theater Operations and Targets*. MS thesis, AFIT/GA/ENY/07-M17. Graduate School of Management and Engineering, Air Force Institute of Technology (AU), Wright-Patterson AFB OH. March 2007.
- Turner, Andrew E. "Constellation Design Using Walker Patterns." AIAA/AAS Astrodynamics Specialist Conference, Monterey, California. August 2002. AIAA Paper 2002- 4904.
- Vallado, D. A., W. D. McClain. *Fundamentals of Astrodynamics and Applications*. New York: The McGraw-Hill Companies, Inc. 1997.
- Walker, John G., "Circular Orbit Patterns Providing Continuous Whole Earth Coverage." Royal Aircraft Establishment Technical Report 70211. November 1970.
- Walker, John G., "Continuous Whole-Earth Coverage by Circular-Orbit Satellite Patterns." Royal Aircraft Establishment Technical Report 77044. 1977.
- Wertz, James R. "Coverage, Responsiveness, and Accessibility for Various 'Responsive Orbits'." AIAA 3rd Responsive Space Conference, Los Angeles, California. April 2005.
- Wertz, James R. *Mission Geometry; Orbit and Constellation Design and Management*. El Segundo: Microcosm Press. 2001.
- Wertz, James R. *Space Mission Engineering: The New SMAD*. El Segundo, Microcosm Press. 2011.
- Wertz, James R., Richard E. Van Allen, Tina Barclay. "NanoEye—Military Relevant Surveillance for Less Than \$5 Million Total Recurring Mission Cost." AIAA 8th Responsive Space Conference, Los Angeles, California. March 2010.
- Wiesel, William E. *Spaceflight Dynamics, Third Edition*. Beavercreek, OH: Aphelion Press. 2010.

Vita

Captain Steven P. Ingraham graduated from Wilmington High School in Wilmington, Ohio, in 2002. He entered undergraduate studies at Embry-Riddle Aeronautical University in Daytona Beach, Florida, where he graduated Magna Cum Laude with a Bachelor of Science in Astronautical Engineering in 2007. He was commissioned through ROTC Detachment 157 as a Distinguished Graduate.

His first Air Force assignment was at Los Angeles Air Force Base as an engineer and Executive Officer in the Spacelift Range Division of the Space and Missile System Center. In August 2011, he entered the Graduate School of Engineering and Management at the Air Force Institute of Technology. After graduating in March 2013 with a Master of Science in Astronautical Engineering, he will be assigned to the Advance Composites Office (AFRL/RX) at Hill Air Force Base, Utah.

REPORT DOCUMENTATION PAGE				Form Approved OMB No. 074-0188	
<p>The public reporting burden for this collection of information is estimated to average 1 hour per response, including the time for reviewing instructions, searching existing data sources, gathering and maintaining the data needed, and completing and reviewing the collection of information. Send comments regarding this burden estimate or any other aspect of the collection of information, including suggestions for reducing this burden to Department of Defense, Washington Headquarters Services, Directorate for Information Operations and Reports (0704-0188), 1215 Jefferson Davis Highway, Suite 1204, Arlington, VA 22202-4302. Respondents should be aware that notwithstanding any other provision of law, no person shall be subject to a penalty for failing to comply with a collection of information if it does not display a currently valid OMB control number.</p> <p>PLEASE DO NOT RETURN YOUR FORM TO THE ABOVE ADDRESS.</p>					
1. REPORT DATE (DD-MM-YYYY) 21-03-2013		2. REPORT TYPE Master's Thesis		3. DATES COVERED (From – To) August 2011 – March 2013	
4. TITLE AND SUBTITLE Dynamic Constellation Tasking and Management				5a. CONTRACT NUMBER	
				5b. GRANT NUMBER	
				5c. PROGRAM ELEMENT NUMBER	
6. AUTHOR(S) Ingraham, Steven P., Captain, USAF				5d. PROJECT NUMBER 13Y162	
				5e. TASK NUMBER	
				5f. WORK UNIT NUMBER	
7. PERFORMING ORGANIZATION NAMES(S) AND ADDRESS(S) Air Force Institute of Technology Graduate School of Engineering and Management (AFIT/ENY) 2950 Hobson Way, Building 640 WPAFB OH 45433-8865				8. PERFORMING ORGANIZATION REPORT NUMBER AFIT- ENY-13-M-18	
9. SPONSORING/MONITORING AGENCY NAME(S) AND ADDRESS(ES) Operationally Responsive Space 2351 Carlisle Blvd. SE, Kirtland AFB, NM 87117-5776 505-853-2413 Dr. Thomas Atwood				10. SPONSOR/MONITOR'S ACRONYM(S) OSD/DOD/ORS	
				11. SPONSOR/MONITOR'S REPORT NUMBER(S)	
12. DISTRIBUTION/AVAILABILITY STATEMENT APPROVED FOR PUBLIC RELEASE; DISTRIBUTION UNLIMITED.					
13. SUPPLEMENTARY NOTES This material is declared a work of the U.S. Government and is not subject to copyright protection in the United States.					
14. ABSTRACT Responsive orbits have gained much attention in recent years and many AFIT theses have addressed this topic. Specifically, the following topics have been studied: phasing within an orbit, adjusting time of arrival, avoidance, and maneuver detection. This thesis seeks to determine the feasibility of maneuvering satellites from circular (600 km) orbits to eccentric (600 km by 175 km) orbits in order to collect high resolution images for Earth surveillance. Coverage is calculated for multiple 6-satellite constellations. Perturbations for the subject orbits are analyzed and compared to simulation results. ΔV requirements are determined to offset the differential perturbations between the circular and eccentric orbits. Additionally, the effects of atmospheric drag are modeled for solar maximum and solar minimum conditions. The ΔV required to offset atmospheric losses is also calculated. Finally, a hypothetical ΔV budget is quantified for a ten day operation and compared to the total ΔV available on the NanoEye concept. The results of this thesis show that maneuvering satellites within a constellation is feasible in order to obtain high resolution images. The ΔV budget for a hypothetical ten day scenario is found to be approximately 1.2 km/s.					
15. SUBJECT TERMS Responsive Orbits, Responsive Constellation, Dynamic Constellation, Maneuvering Spacecraft					
16. SECURITY CLASSIFICATION OF:			17. LIMITATION OF ABSTRACT UU	18. NUMBER OF PAGES 122	19a. NAME OF RESPONSIBLE PERSON Black, Jonathan T., PhD USAF ADVISOR
a. REPORT U	b. ABSTRACT U	c. THIS PAGE U			19b. TELEPHONE NUMBER (Include area code) (937) 255- 3636 ext 4578

